



HAL
open science

Evidencing the chemical degradation of a hydrophilized pes ultrafiltration membrane despite protein fouling

Murielle Rabiller-Baudry, Aurélie Bouzin, Charlène Hallery, Jean Girard,
Cindy Leperoux

► **To cite this version:**

Murielle Rabiller-Baudry, Aurélie Bouzin, Charlène Hallery, Jean Girard, Cindy Leperoux. Evidencing the chemical degradation of a hydrophilized pes ultrafiltration membrane despite protein fouling. *Separation and Purification Technology*, 2015, 147, pp.62-81. 10.1016/j.seppur.2015.03.056 . hal-01141490

HAL Id: hal-01141490

<https://univ-rennes.hal.science/hal-01141490>

Submitted on 4 Nov 2015

HAL is a multi-disciplinary open access archive for the deposit and dissemination of scientific research documents, whether they are published or not. The documents may come from teaching and research institutions in France or abroad, or from public or private research centers.

L'archive ouverte pluridisciplinaire **HAL**, est destinée au dépôt et à la diffusion de documents scientifiques de niveau recherche, publiés ou non, émanant des établissements d'enseignement et de recherche français ou étrangers, des laboratoires publics ou privés.

**EVIDENCING THE CHEMICAL DEGRADATION OF A HYDROPHILIZED PES
ULTRAFILTRATION MEMBRANE DESPITE PROTEIN FOULING**

Murielle RABILLER-BAUDRY*, Aurélie BOUZIN, Charlène HALLERY, Jean GIRARD,
Cindy LEPEROUX

1-Université de Rennes 1, « Institut des Sciences Chimiques de Rennes » UMR-CNRS 6226,
263 avenue du Général Leclerc, CS 74205, case 1011, 35042 Rennes cedex, France

Corresponding author: murielle.rabiller-baudry@univ-rennes1.fr

KEYWORDS

PES, PVP, ultrafiltration, proteins, ageing, hypochlorite, FTIR-ATR

ABSTRACT

Hydrophilisation of polyethersulfone (PES) based membrane is often achieved by addition of polyvinylpyrrolidone (PVP) leading to a physical blend of the two polymers. This paper shows that the most commonly used membrane for UF in dairy industry is a PES/PVP based one. Nevertheless if hydrophilisation limits the organic fouling, PVP is also the Achilles heel of these membranes. It is particularly true when membranes are exposed to hypochlorite as it is the case for cleaning/disinfection steps. Evidencing the disappearance of PVP from a pristine PES/PVP membrane can be easily achieved by FTIR-ATR analyses. But when one wants to study the ageing of a membrane used in UF it gets more complicated: regardless of the cleaning efficiency the membrane always remains fouled by some proteins. As both PVP and proteins own chemical bounds leading to absorption at the same wavenumber in FTIR-ATR, it thereby prevents the easy highlighting of the PVP degradation. The aim of this paper is to propose a simple treatment of raw FTIR-ATR spectra to dissociate these two contributions, allowing consequently the study of the degradation of a fouled membrane. Then the procedure is applied to a real case study on a spiral membrane.

1. INTRODUCTION

Fouling systematically occurs during ultrafiltration (UF) as it is observed when filtering skim milk by spiral membranes based on polyethersulfone (PES, **Figure 1**) [1-4]. The membrane composition is of course an important parameter as the physico-chemical interactions between the skim milk components and the membrane material play a crucial role on the membrane global fouling [5]. In fact, PES membranes also contained a minor amount of additives that are added to increase the membrane hydrophilic character, but generally these additives are not clearly mentioned by the membrane providers. Polyvinylpyrrolidone (PVP) (**Figure 1**) is one of the most famous used additive and it is quite logical to suspect its presence in a hydrophilised PES membrane. But it must generally be proved as it will be done in this study as preliminary investigation (see results).

Nowadays, it is quite well understood that hydrophilisation limits the membrane fouling by organic compounds such as proteins. Nevertheless, it is also known that PVP is the Achilles heel of these membranes. This is particularly true when they are exposed to sodium hypochlorite (NaOCl) as it is the case for daily cleaning/disinfection steps at industrial scale.

To go ahead in the understanding in PES/PVP membrane stability, several teams working in membrane food or water applications have chosen to study variations of flux and selectivity after immersion of pristine membranes in various NaOCl solutions. For such purposes they used more or less complex degradation protocols [2, 6, 8-22].

Dealing with the membrane material degradation, in our opinion one of the most comprehensive fundamental results is obtained by infra-red analyses (FTIR). Infra-red spectroscopy is a technique only able to evidence polar bounds existing in polymers. Nevertheless it must be underlined that these studies are achieved on pristine membranes that were voluntarily aged in sodium hypochlorite solutions, the pH of which is generally set in the range 8.0 – 9.0. NaOCl disinfecting solutions having such pHs are known to be lead to severe degradation of PES/PVP membranes [see for instance 18, 19 and references cited herein].

In the case of PES/PVP membranes a special attention must be paid to an absorption band of the FTIR-ATR spectrum located close to a wavenumber at 1661 cm^{-1} and attributed to the C=O amide bound of PVP. To put it in a nutshell, the PVP C=O bound progressively disappears during the membrane ageing provoked by NaOCl treatments. **Figure 2** shows one

of the mechanism suggested in literature to explain the C=O disappearance that can be understood as the opening of the PVP ring. This is significantly different from a total removal of the PVP or of its degradation compounds.

Moreover, another band located at 1030 cm^{-1} progressively appears on the FTIR-ATR spectrum and is commonly attributed to an evolution of the PES skeleton itself. Nevertheless there is still controversy about the exact meaning of this band, sometimes assigned to a sulfonic acid group (SO_3H , **Figure 3a**, [14]) and recently to a phenol formation (OH on phenyl ring, **Figure 3b**, [18]). It is out of the scope of this paper to discuss the validity of these two proposal and in the following we will only discuss degradation of PES skeleton evidenced by the 1030 cm^{-1} band without any other comments.

To show the evolution of the PES skeleton is quite easy on an aged membrane that have been used at industrial scale because no band overlapping have been evidenced with the fouling (**Figure 4**) and the 1030 cm^{-1} is a pure signal revealing the PES degradation. For a more detailed presentation of the membrane used at industrial scale and called here “Membrane U” see [1].

The disappearance of PVP from a pristine PES/PVP membrane can be easily achieved by FTIR-ATR analysis, but only a single band can be used for this purpose: those located at 1661 cm^{-1} . But when one wants to study the ageing of a membrane used in UF it gets more complicated because of the presence of fouling as it will be explained below.

Dealing with PES/PVP membranes fouled during UF of skim milk, it must be underlined that only a part of the whole fouling is irreversible (not removed by a simple water rinsing) and this part is known to be made of proteins only, in the particular case of organic membranes [3-4]. This irreversible protein deposit represents the target of the cleaning/disinfecting operation that immediately follows the production step. Classically, at industrial scale, organic UF membranes fouled by skim milk are cleaned according to a procedure involving a cascade of 3 solutions set at 50°C : alkaline cleaning at pH 11.5/12.0 with a formulated detergent containing surfactants, then acid cleaning generally with nitric acid at pH 1.6 and finally an alkaline and chlorine disinfecting step using sodium hypochlorite (bleach) set at 150-200 ppm in total free chlorine (TFC) [1, 3, 4]. In our previous studies we have explained how such a cascade can be simplified by the cancellation of the acid step [7]. Nevertheless for food security purposes it is not possible to withdraw the disinfecting step. Physico-chemical

analyses of such industrial membranes autopsied at the end of their service life highlight presence of a residual protein fouling even after a final cleaning procedure [1].

Proteins own a specific bound called “amide I” (C=O vibration of the amide group, -CO-NH) that is superimposed to the PVP C=O bound (the only one that can be used to deal with the PVP degradation). Consequently, an analytical difficulty must be overcome when fouling is made of proteins (**Figure 5**) to unambiguously evidence modifications of the membrane due to fouling occurrence or to membrane material degradation or a combination of the two.

So in this paper we propose an approach to treat a FTIR-ATR spectrum in order to dissociate the contributions of PVP and proteins to the global band obtained on the raw spectrum of a fouled membrane. For the demonstration pristine membranes at 3 degradation states are prepared and fouled with proteins. Then the methodology is applied to the analysis of a spiral membrane (6.7 m²) used at laboratory scale alternatively in UF of skim milk and UF of sodium hypochlorite aiming at evidencing a possible heterogeneity of the membrane degradation with respect to the distribution of fouling in this complex geometry.

2. THEORETICAL PART

On the FTIR-ATR spectra of a PES/PVP pristine membrane (here HFK-131 membrane) all bands can be assigned to PES except that located at 1661 cm⁻¹ which can be attributed to the C=O bound of PVP. **Figure 4** shows the attributions in the 1770-700 cm⁻¹ range that is the range of interest for the following discussion. For sake of comparison, the spectrum of a membrane already used at industrial scale (Membrane U) is also given. Membrane U is at the end of its service life that corresponds to 8,000 h of skim milk UF. A final and very efficient cleaning has been performed before the FTIR-ATR spectrum registration. As explained in the introduction, clearly the PVP C=O band has disappeared and the new 1030 cm⁻¹ band has appeared on the spectrum.

However, when the membrane is fouled by milk proteins and when the cleaning is not sufficiently efficient to remove the proteins from the membrane, the PVP C=O band and the amide I band of proteins are overlapped. This analytical difficulty would be more and more frequent with the membrane ageing because the fouling tends to increase with the membrane age and the cleanability seems to decrease accordingly. **Figure 5** shows the raw spectra obtained for a pristine membrane and for a protein fouled one. If the protein deposit is very

high (see results) then an aged and fouled membrane can exhibit a C=O band of greater intensity than that of the pristine membrane itself. Consequently it becomes impossible to deal with a possible degradation of PVP from the membrane without any treatment of the FTIR-ATR spectrum.

We propose to establish a mathematical treatment of the spectrum in order to dissociate the contribution of these two C=O bands. Moreover, this paper aims at developing a simple approach that can be applied without any sophisticated and costly software able to perform band deconvolution.

Proteins also lead to a second characteristic absorption band called amide II band that corresponds to the superimposition of vibrations due to CN+NH bounds of the amide group.

Knowing that the protein amide II band, located close to 1539 cm^{-1} , have no overlapping with the pristine membrane bands, neither PES nor PVP, we have already developed a method of quantification of proteins directly on the HFK-131 membrane. This analysis is based on the $H_{1539}^{\text{protein amide II}} / H_{1240}^{\text{PES}}$ ratio (with H_i^X : band height corresponding to the absorbance intensity at a given i wavenumber (w_i) and corresponding to X material or functional group) [4].

The first step of the approach proposed in this paper is based on the simple fact that on a fouled membrane, absorption measured at 1661 cm^{-1} ($H_{1661}^{\text{raw spectrum}}$) corresponds to the superimposition of absorbance due to PVP (H_{1661}^{PVP}) and absorbance due to protein amide I vibration ($H_{1661}^{\text{protein amide I}}$):

$$H_{1661}^{\text{raw spectrum}} = H_{1661}^{\text{PVP}} + H_{1661}^{\text{protein amide I}} \quad (\text{eq. 1})$$

The new idea of this paper consists in the determination of the protein amide I intensity at 1661 cm^{-1} ($H_{1661}^{\text{protein amide I}}$) from that of the amide II band ($H_{1539}^{\text{protein amide II}}$).

As mentioned previously, these two bonds belong to the same amide group, namely N-C=O, but correspond to different vibration modes. Consequently it is not creasy to imagine that the intensity of the two FTIR bands of the amide group of proteins are correlated. Assuming this idea, we have tried to evidence the possible relationship between the two heights of these bounds without any other assumption. The experimental developments detailed in the results

show that the relationship between the two heights exists. Moreover experimental results evidence that, regardless of the chosen protocol, the relationship is linear (see below). For sake of simplification the general form of this relationship is consequently given as that of a straight line (**equation 2**).

$$H_{1661}^{\text{protein amide I}} = \alpha H_{1539}^{\text{protein amide II}} + \beta \quad (\text{eq. 2})$$

Where α and β are coefficients to be determined.

A main bottleneck of the approach is the experimental determination of α and β . In the results we will discuss two experimental approaches to determine these coefficients. One is based on spectra acquired for proteins in aqueous solutions. The other involved treatment of spectra acquired with more or less aged membranes on which controlled protein deposit are made. It is explained in the results why only one of these two approaches can be validated.

The second key point is the experimental validation of **equation 3** that can be easily drawn from the previous ones.

$$H_{1661}^{\text{raw spectrum}} / H_{1240}^{\text{PES}} = (H_{1661}^{\text{PVP}} / H_{1240}^{\text{PES}}) + (H_{1661}^{\text{protein amide I}} / H_{1240}^{\text{PES}}) \quad (\text{eq. 3})$$

It requires having PES/PVP membranes with various amount of PVP. In this paper we have used pristine and aged membranes specially prepared to cover a wide range of membrane degradation up to a PVP height divided by two with respect to its initial height.

Figure 6 summarizes the global approach.

3. EXPERIMENTAL

3.1.1. Water, skim milk and solutions

Water used either for solution preparation and membrane rinsing is deionised and 1 μm filtered. Its conductivity is always lower than 1 $\mu\text{S}\cdot\text{cm}^{-1}$.

The skim milk used is a commercial one (UHT, Lait de Montagne, Carrefour, France) containing an average of 32 g.L⁻¹ proteins and 48 g.L⁻¹ carbohydrates (mainly lactose) and only traces of lipids (< 0.5 %).

Protein solutions are prepared from a powder containing whey proteins (PS90 Protarmor, Saint Brice en Coglès, France) dissolved in deionised water. A set of 6 concentrations is used: 0, 5, 10, 20, 30 and 50 g.L⁻¹.

NaOCl solutions at 400 ppm in total free chlorine (TFC) are prepared from commercial bleach solution provided by Lacroix (eau de Javel, bleach at 96,000 ppm TFC, France). The pH is adjusted to 8.0 ± 0.1 by addition of HCl of analytical grade (Acros).

A formulated alkaline solution, namely P3-ultrasil 10 provided by Ecolab (Issy les Moulineaux, France) is used for membrane cleaning. It is set at 4 g.L⁻¹ that corresponds to a natural pH of 12.0.

3.1.2. Membranes

The membrane used is named HFK-131. It is a UF membrane provided by Koch (USA) and commonly used at industrial scale for UF of skim milk and of both acid and rennet whey. This membrane represents about 70 % of the world market for these specific applications. It is a PES based membrane of 5-10 kg mol⁻¹ molecular weight cut off according to the provider.

We have studied this membrane to prove that it is a PES/PVP one. Among experimental data allowing to draw this conclusion are:

- (i) the presence of the 1661 cm⁻¹ band on the FTIR-ATR spectra (**Figure 4, Figure 5**). Moreover, we had also checked that the HFK-131 spectrum is similar to that of a dense film we had prepared, that was made from PES and PVP physical blend (95/5) [6].
- (ii) the presence of nitrogen evidenced by nano-SIMS measurements (**Figure 7**). SIMS is only able to evidence nitrogen atoms bounded to carbon further called organic nitrogen (CN group).

3.1.2.1. Spiral membrane

The spiral membrane is chosen in order to have a filtering area of several square meters (6.7 m², 4333 K131 VYV module). The membrane (further called CIP-3, KMS K131V 8879759136) is made of 4 double sheets of membranes wound around a permeate collector tube of 33 inches length as schematically explained in **Figure 8**.

3.1.2.2. Flat membrane coupons: fouling of pristine and aged membranes

Several flat membranes of 127 cm² (or sometimes less) are sampled in a second pristine spiral membrane (further called cut-CIP-1). These membrane coupons are used for FTIR-ATR analyses performed to validate the methodological approach explained in the theoretical part. Prior to be used these samples are carefully rinsed in water to remove the preservative (the rinsing efficiency is systematically checked by FTIR-ATR).

- Ageing of membrane coupons

The ageing protocol is inspired from the one established in our laboratory and already described in [6]. Six membrane coupons (6 cm x 3 cm) are soaked in a NaOCl solution set at 400 ppm TFC and pH 8.0 (V= 26.3 mL, surface/volume = 14.6 L.m⁻²) under micro-waves (pulsed microwaves at 255 W) during 210 or 480 min. The micro-waves help to accelerate the chemical degradation when compared to simple soaking in the same solution. Thus depending on the treatment duration different ageing states are reached; it is shown from the PVP C=O height decrease. In order to avoid impact of NaOCl concentration during the ageing process, the NaOCl solution has been regularly replaced by a similar volume of a fresh solution. Some characteristics of aged membranes are given **Table 1**.

- Protein fouling of membrane coupons

The protocol is the same when using pristine and aged membranes. A membrane coupon (3 cm x 6 cm) is immersed under gentle stirring at room temperature in 100 mL of a protein solution during 2 h. Proteins are set at different concentrations (0, 5, 10, 20, 30 and 50 g.L⁻¹). After dripping, membranes are carefully dried in a desiccator under dynamic vacuum. FTIR-

ATR spectrum is registered on each dried coupon before and after the protein deposition. Protein quantification is achieved using **equation 4** (see below). The amount of proteins on obtained deposit are shown **Table 1** for the pristine membrane and the two aged membranes.

3.1.3. UF with the spiral membrane

3.1.3.1. Skim milk UF

A pristine spiral membrane is installed on a pilot provided by TIA (TIA 3093, Bollène, France) and already described in [24]. The fouling of the spiral membrane is achieved by UF of 24 L of skim milk at 50°C in batch mode at volume reduction ratio VRR= 1, meaning here that both the retentate and the permeate are fully recycled in the feed tank. During UF the feed flow rate is constant. It is set at $9.5 \text{ m}^3 \cdot \text{h}^{-1}$ that corresponds to a cross-flow velocity of about $0.3 \text{ m} \cdot \text{s}^{-1}$.

The transmembrane pressure (TMP) is regularly increased from 1.5 bar at start to 4.0 bar at the end of the UF run. This last TMP value allows to reach the limiting flux. Each TMP increase is achieved when a plateau value of flux is reached at the previous TMP. The UF duration is close to 5.5 h for one UF run. The membrane flux (J) is followed all over the skim milk UF.

The average TMP is classically calculated as the mean value when considering the membrane inlet and outlet TMPs. Nevertheless, it must be kept in mind that the pressure drop along the membrane element is 2.2 bar regardless of the average TMP. This is not a negligible value by comparison to the average TMP itself. In the following an estimation of the local TMP is made considering a linear pressure drop along the membrane element, according to a calculation proposed in [23].

At the end of skim milk UF, the membrane is extensively rinsed by water. Then it is cleaned at 2 bar, 50°C during 1 h by 25 L of P3-ultrasil 10 formulated solution. This protocol allows the water flux recovery of the pristine membrane.

3.1.3.2. Sodium hypochlorite UF for membrane ageing

In order to accelerate the spiral membrane ageing, UF of sodium hypochlorite solution at 400 ppm TFC and pH 8.0 is performed at 2.0 bar and 50°C. The treatment duration can vary and is summarized as a cumulative dose of hypochlorite expressed according to **equation 5**.

$$\text{NaOCl}_{\text{dose membrane exposition}} (\text{ppm.d}) = 400 \text{ ppm} \times \text{number of days} \quad (\text{eq. 4})$$

From a practical point of view, 3 UF of skim milk are consecutively performed on the pristine membrane. After alkaline cleaning the membrane is then aged in NaOCl up to a cumulative dose of 400 ppm.d. Then another UF of skim milk is performed. After a second alkaline cleaning the membrane is aged in NaOCl up to a cumulative dose of 2,000 ppm.d. Then another UF of skim milk is performed. After cleaning the membrane is aged up to a cumulative dose of 2,800 ppm.d and a final skim milk UF is performed. Finally, the membrane is carefully rinsed by water but not cleaned. Then the membrane is autopsied.

According to the provider this membrane is guaranteed up to a 5,000 ppm.d NaOCl dose but nothing is clearly explained about the way to reach this dose. Nevertheless, we can suggest that the autopsied CIP-3 membrane could be equivalent to a membrane close to half time of a normal service life at industrial scale.

3.1.4. FTIR-ATR on membranes for protein quantification purpose

The membrane samples are carefully dried under dynamic vacuum before registration to remove water (systematically checked in the 3500 cm⁻¹ region).

For sake of generalization, three different FTIR-ATR spectrometers have been used in this study. Their characteristics are shown in **Table 2** as well as the standard conditions used for spectra acquisition. It has been checked that the spectra acquired on each spectrometer are similar when dealing with the wavenumbers but the raw intensity of each band is different. This is probably due to differences in the ATR-accessory crystal (chemical nature and reflection number). Nevertheless it has also been checked that the relative ratio of two band heights (for instance: $H_i/H_{1240}^{\text{PES}}$) are the same regardless of the spectrometer used (see **Figure A1** in Appendix 1).

3.1.4.1. Quantification of residual proteins directly on membranes

The initial calibration has been established with spectrometer 1 [3, 4, 6] but as explained above can be used with spectrometer 2 (see **Figure A1** in Appendix 1) and spectrometer 3.

The quantification is possible in a wide range of fouling from 1 to 350 μg of proteins per square centimetre of membrane (geometric area) with a precision of 1 $\mu\text{g}\cdot\text{cm}^{-2}$ (**equation 4**).

19 samples of fouled pristine membranes have been used to establish the equation, allowing to reach $r^2 = 0.997$.

$$H_{1539}^{\text{protein amide II}} / H_{1240}^{\text{PES}} - H_{2060-2240}^{\text{baseline}} = 0.0034 [\text{P}] \quad (\text{eq. 4})$$

With:

[P]: the protein concentration in $\mu\text{g}\cdot\text{cm}^{-2}$

H_i^X : band height corresponding to the absorbance intensity at a given wavenumber (w_i) and corresponding to X material or functional group. (see **Appendix 1**).

$H_{2060-2240}^{\text{baseline}}$: the average height of the baseline measured in the 2060-2240 cm^{-1} range of wavenumbers. Value equal to 0.0165.

- Specific procedure for the spiral membrane

After the final fouling by skim milk up to 4.0 bar and rinsing by deionised water, the spiral membrane (CIP-3, 6.7 m^2) has been cut in 324 pieces of about 127 cm^2 area each.

Each flat sample is then analyzed with spectrometer 1. Only the spectrum of the sample center is registered. Nevertheless, each 127 cm^2 sample could be divided in 9 smaller pieces of about 10 cm^2 (corresponding to the ZnSe crystal area), but it has been checked on a whole membrane sheet of about 1 m^2 that the variations are not significant and that a single result seems quite acceptable for the followed purpose.

This autopsy allows establishing firstly the mapping of the irreversible fouling and secondly that of the degradation state of the membrane by the mean of measurements at 1661 cm^{-1} (PVP) and 1030 cm^{-1} (PES skeleton).

- Specific procedure for the flat membrane coupons

The small flat membrane coupons have been analyzed with spectrometer 2. It was used to establish the protocol exposed in the theoretical part above.

3.1.5. FTIR-ATR on membranes for evidencing of membrane degradation

Firstly the spectrum of each membrane coupon, in pristine form, is registered. Thus H_{1240}^{PES} and H_{1661}^{PVP} is measured allowing the calculation of the $H_{1661}^{PVP}/H_{1240}^{PES}$ ratio for each sample.

Secondly, some membrane coupons are submitted to a more or less intensive ageing procedure according to the protocols described in paragraph 3.1.2. Then the spectrum of each aged membrane coupon is registered. Thus H_{1240}^{PES} and H_{1661}^{PVP} is measured allowing the calculation of the $H_{1661}^{PVP}/H_{1240}^{PES}$ ratio for each sample before fouling. Of course it has been checked that the PVP band is modified when compared to that measured before the ageing treatment. These values obtained after ageing are then used as reference values to be compared to values obtained after fouling on aged membranes.

Finally, membranes are fouled with protein solutions according to the protocol described in paragraph 3.1.2. FTIR-ATR spectra are then registered and $H_{1661}^{raw\ spectra}$, H_{1240}^{PES} and $H_{1661}^{protein\ amide\ II}$ are determined for the registered spectrum of each membrane coupon after fouling allowing the acquisition of the raw spectra of aged then fouled membranes.

The following ratios, $H_{1661}^{raw\ spectra}/H_{1240}^{PES}$ and $H_{1661}^{protein\ amide\ II}/H_{1240}^{PES}$ can easily be deduced. Then $H_{1661}^{protein\ amide\ I}/H_{1240}^{PES}$ of the fouled membrane is drawn from **equation 3** with the $H_{1661}^{raw\ spectra}/H_{1240}^{PES}$ ratio of the fouled membrane and the $H_{1661}^{PVP}/H_{1240}^{PES}$ ratio of the same coupon before fouling.

Finally the $H_{1661}^{protein\ amide\ I}/H_{1661}^{protein\ amide\ II}$ ratio is obtained from the $(H_{1661}^{protein\ amide\ I}/H_{1240}^{PES})$ to $(H_{1661}^{protein\ amide\ II}/H_{1240}^{PES})$ ratio.

3.1.6. FTIR-ATR on protein solutions

Spectra of 1 μ L of the several protein solutions have been registered with spectrometer 2.

The obtained spectrum of a solution (Protein raw spectrum) is the superimposition of the water spectrum and of the protein one. But because the main component of a protein solution is water that have a band located at 1637 cm^{-1} which overlaps the amide I band of proteins, a treatment of the raw spectrum is needed to put in evidence amide I and amide II bands of proteins (**Equation 6**, see **Appendix 2** for details). After treatment the spectrum is called Protein difference spectrum

$$\text{Protein difference spectrum} = \text{Protein raw spectrum} - \gamma \text{water spectrum} \quad (\text{eq. 6})$$

With:

γ coefficient to be determined for each protein spectrum. The determination of γ is based on the cancellation of the OH band of water located close to 3300 cm^{-1} . There is no significant overlapping of the 3300 cm^{-1} water band with protein bands in this region, because unsaturated C-H bonds of proteins are located below 3000 cm^{-1} . The determination of γ is the result of tests and errors with different values close to 1.000 with the objective to obtain a region close to 3300 cm^{-1} as flat as possible in the Protein difference spectrum that is the considered criterion to prove the quality of the spectrum treatment. Moreover, for similar reason, the $2300\text{-}1800\text{ cm}^{-1}$ region must also be as flat as possible on the difference spectrum (see **Appendix 2** for details). From a practical point of view, in this study γ slightly varies around 0.8 ± 0.2 .

4. RESULTS AND DISCUSSION

4.1. FTIR-ATR study of estimation of protein amide I band from protein amide II band

As already explained the first bottleneck of the procedure (**Figure 6**) consists in the estimation of protein amide I intensity from that of protein amide II on the FTIR-ATR spectrum. Two approaches have been tested that are detailed in the following.

4.1.1. Proteins in solution

Spectra of $1\text{ }\mu\text{L}$ of several protein solutions have been registered with spectrometer 2. Spectra have then been post-treated according to the procedure described in paragraph 3.1.6.

The results evidence that the $H_{1661}^{\text{protein amide I}} / H_{1539}^{\text{protein amide II}}$ ratio decreases linearly with protein concentration according to **equation 7**.

$$H_{1661}^{\text{protein amide I}} / H_{1539}^{\text{protein amide II}} = - 0.06 \times [P'] + 3.6 \quad \text{with } r^2 = 0.95 \quad (\text{eq. 7})$$

With:

[P'] the concentration of proteins in g.L^{-1}

This linear trend suggests a structural evolution of proteins with dilution.

4.1.2. Proteins adsorbed on flat membrane

Spectra of voluntary aged and fouled membrane coupons have been registered with spectrometer 1. Then spectra have been post-treated according to the procedure described in paragraph 3.1.5.

Table 3, **Table 4** and **Table 5** present FTIR-ATR data before and after fouling by proteins on the pristine membrane and the two aged ones.

Whatever the fouling amount and the membrane ageing state, the $(H_{1661}^{\text{protein amide I}} / H_{1240}^{\text{PES}})$ ratio is always proportional to the $(H_{1539}^{\text{protein amide II}} / H_{1240}^{\text{PES}})$ ratio; this means that $\beta=0$ in **equation 2**.

Moreover, the $(H_{1661}^{\text{protein amide I}} / H_{1539}^{\text{protein amide II}})$ ratio, and thus α term of **equation 2**, is the same for the three aged state membranes in a wide range of protein deposit amount. (**Table 6**).

4.1.3. Conclusion on the two approaches

Estimation of the height of protein amide I band from the height of protein amide II band can be achieved from spectra acquired with proteins in solution and with proteins adsorbed on membranes. Nevertheless the conclusions are clearly different: in solution the ratio of the two band heights varies whereas it remains constant for proteins adsorbed on membranes.

In solution, this result suggests a structural evolution of proteins with dilution likely due to a competition between hydrogen bond due to protein-protein interactions and those due to protein-water interactions.

On membranes, adsorption is mainly due to hydrophobic interactions that lead to similar structures of adsorbed proteins, regardless of the amount that always remains low.

Finally the proposed approach can be validated by using calibration obtained with protein adsorbed on membranes because it is a closer situation to that of adsorbed proteins during UF (**Table 6**).

4.2. Spiral membrane degradation state

The degradation state is discussed from both flux measurements and FTIR-ATR spectra.

4.2.1. UF of skim milk

For pristine CIP-3 membrane, the permeability to water at 50°C is 59.8 L.h⁻¹.m⁻².bar⁻¹.

Three UF of skim milk have been performed on the pristine membrane with an alkaline cleaning step between each of them. **Figure 9** shows the excellent reproducibility.

After a sufficient dose of NaOCl received by the membrane, fluxes progressively increase, highlighting, on a hydrodynamic point of view, that membrane degradation occurs. It is also evidenced that more than the limiting flux the critical flux also varies with the membrane ageing (see [24] and references cited herein for a discussion dealing with limiting and critical fluxes with the pristine membrane in skim milk).

4.2.2. Mapping of the protein irreversible deposit

After the last skim milk UF (NaOCl dose set at 2,800 ppm.d) the membrane is rinsed and autopsied. **Figure 10** shows the distribution of the residual protein amount according to the location on the eight membrane sheets (supporting values are given **Figure A4-1** in Appendix

4). The zone closed to the permeate collector axis is often more fouled. An average value is calculated on all the membrane and corresponds to $50 \pm 9 \mu\text{g}\cdot\text{cm}^{-2}$.

4.2.3. PVP distribution on aged and fouled membrane

Figure 11 shows the mapping of the $(H_{1661}^{\text{raw spectra}}/H_{1240}^{\text{PES}})$ ratio as determined from raw spectra obtained by FTIR-ATR. An average ratio is calculated on the whole membrane corresponding to 0.24 ± 0.03 (RSD = 11 %, the supporting values can be seen in **Figure A4-2** in **Appendix 4**).

Figure 12 shows the mapping of the $(H_{1661}^{\text{PVP}}/H_{1240}^{\text{PES}})$ ratio as determined from raw spectra obtained by FTIR-ATR and applying **equation 3**. An average ratio is calculated on the whole membrane corresponding to 0.08 ± 0.02 (RSD = 18 %, the supporting values can be seen in **Figure A4-3** in **Appendix 4**). The PVP amount can be roughly considered as constant, highlighting a regular, but not total, disappearance of PVP on the whole membrane. This value is between that of the pristine membrane (0.14) and that of the industrial aged membrane (membrane U after extensive cleaning, 0.06).

In this spiral membrane, the protein amount varies from 10 to $80 \mu\text{g}$ of proteins per cm^2 but most values are in the range $40\text{-}60 \mu\text{g}\cdot\text{cm}^{-2}$: fouling is not homogeneous whereas the PVP amount appears roughly constant. Consequently it is not possible to evidence if the protein fouling plays a protective role toward the PVP degradation. Nevertheless it is not possible to conclude on the absence of this protection.

4.2.4. PES degradation on aged and fouled membrane

PES degradation has been checked from the 1030 cm^{-1} band increase. **Figure 13** shows the mapping of the $(H_{1030}/H_{1240}^{\text{PES}})$ ratio as determined from raw spectra obtained by FTIR-ATR. An average ratio has been calculated on the whole membrane corresponding to 0.13 ± 0.06 even if the relative standard deviation is very high (RSD = 45 %, the supporting values can be seen in **Figure A4-4** in **Appendix 4**). Consequently, this degradation state cannot be considered as constant and further investigations are needed to understand the origin of this observation. Nevertheless all these values are significantly lower than that of the industrial aged membrane (Membrane U after extensive cleaning, 0.29).

For similar reasons, it is not possible to evidence if the protein fouling plays or not a protective role toward the PES degradation.

Prulho et al. [19] and Pellegrin et al. [20] suggested a link between PVP degradation and PES degradation. These authors believe that some degradation compounds of PVP obtained from reaction involving NaOCl can be active organic radicals. These radicals would be able to attack the PES skeleton and lead to the 1030 cm^{-1} band. So we tried to find correlation between PVP disappearance ($H_{1661}^{\text{PVP}}/H_{1240}^{\text{PES}}$) and PES degradation ($H_{1030}/H_{1240}^{\text{PES}}$). But no particular relationship was found (see **Figure A3-1** in Appendix 3). Our results were not able to confirm nor infirm the assumption of these authors.

CONCLUSION

This paper proposes and validates an approach to evaluate the degradation state of a PES/PVP membrane even when the membrane is fouled by proteins.

The procedure is based on FTIR-ATR technique and can be used with spectrometers of different characteristics aiming at a generalization of these results.

The approach is then successfully applied to a case study of a spiral membrane voluntarily aged on a UF pilot by filtration of a 400 ppm NaOCl pH 8.0 solution alternatively with UF of skim milk.

Mapping of the irreversible fouling distribution in this membrane aged at 2,800 ppm.d NaOCl dose has been performed. The results demonstrate the existence of a protein distribution that is different from that observed at lower TMP with a pristine membrane [24]. The PVP remaining amount is quite regular showing a partial degradation but not a total disappearance. The PES skeleton is also degraded but in a more irregular way. An attempt of correlation between protein fouling and PVP disappearance or PES degradation failed. Nevertheless it is not possible to draw conclusion about the efficiency or the non-efficiency of protection of the fouling layer toward the whole process of membrane degradation. Moreover, it has not been possible to evidence a link between PVP disappearance and PES skeleton degradation.

ACKNOWLEDGEMENTS

This study was financially supported by the French ANR program “Méduse” (project n° ANR-09-BLAN-0055-01).

The authors acknowledge Thomas DELHAYE, from University of Rennes 1 (Nanosims Platform) for the SIMS analysis of the pristine membrane.

The authors acknowledge Frederic Bon from University of Rennes 1- IUT Rennes for discussion.

ACCEPTED MANUSCRIPT

REFERENCES

- [1] L. Begoin, M. Rabiller-Baudry, B. Chaufer, C. Faille, P. Blanpain-Avet, T. Benezech, T.A. Doneva, Methodology of analysis of a spiral wound module. Application to PES membrane of ultrafiltration of skimmed milk, *Desalination* 192 (2006) 40-53.
- [2] L. Begoin, M. Rabiller-Baudry, B. Chaufer, M.C. Hautbois, T.A. Doneva, Ageing of PES industrial spiral-wound membranes in acid whey ultrafiltration, *Desalination* 192 (2006) 25-39.
- [3] M. Rabiller-Baudry, L. Bégoïn, D. Delaunay, L. Paugam, B. Chaufer, A dual approach of membrane cleaning based on physico-chemistry and hydrodynamics: Application to PES membrane of dairy industry, *Chem. Eng. Process.* 47 (2008) 267-275.
- [4] D. Delaunay, M. Rabiller-Baudry, J.M. Gozálvez-Zafrilla, B. Balannec, M. Frappart, L. Paugam, Mapping of protein fouling by FTIR-ATR as experimental tool to study membrane fouling and fluid velocity profile in various geometries and validation by CFD simulation, *Chem. Eng. Process.* 47 (2008) 1106–1117.
- [5] H. Bouzid, M. Rabiller-Baudry, L. Paugam, F. Rousseau, Z. Derriche, N.E. Bettahar, Impact of zeta potential and size of caseins as precursors of fouling deposit on limiting and critical fluxes in spiral ultrafiltration of modified skim milks, *J. Membr. Sci.* 314 (2008) 67-75.
- [6] M. Rabiller-Baudry, C. Leperoux, D. Delaunay, H. Diallo, L. Paquin, On the use of microwaves to accelerate ageing of an ultrafiltration PES membrane by sodium hypochlorite to obtain similar ageing state to that obtained for membranes working at industrial scale, *Filtration* 14 (2014) 38-48.
- [7] L. Paugam, D. Delaunay, N.W. Diagne, M. Rabiller-Baudry, Cleaning of skim milk PES ultrafiltration membrane: on the real effect of the cleaning acid step, *J. Membr. Sci.* 428 (2013) 275-280.

[8] C. Causserand, S. Rouaix, J.P. Lafaille, P. Aimar, Degradation of polysulfone membranes due to contact with bleaching solution, *Desalination* 199 (2006) 70-72.

[9] S. Rouaix, C. Causserand, P. Aimar, Experimental study of the effects of hypochlorite on polysulfone membrane properties, *J. Membr. Sci.* 277 (2006) 137-147.

[10] F. ThomINETTE, O Farnault, E. Gaudichet-Maurin, C. Machinal, J.C. Schrotter, Ageing of polyethersulfone ultrafiltration membranes in hypochlorite treatment, *Desalination* 200 (2006) 7-8.

[11] E. Gaudichet-Maurin, F. ThomINETTE, Ageing of polysulfone ultrafiltration membranes in contact with bleach solutions, *J. Membr. Sci.* 282 (2006) 198-204.

[12] E. Arkhangelsky, D. Kuzmenko, V. Gitis, Impact of chemical cleaning on properties and functioning of polyethersulfone membranes, *J. Membr. Sci.* 305 (2007) 176-184.

[13] C. Causserand, S. Rouaix, J.P. Lafaille; P. Aimar, Ageing of polysulfone membranes in contact with bleach solution: Role of radical oxidation and of some dissolved metal ions, *Chem. Eng. Process.: Process Intensification* 47 (2008) 48-56.

[14] K. Yadav, K.R. Morison, M.P. Staiger, Effects of hypochlorite treatment on the surface morphology and mechanical properties of polyethersulfone ultrafiltration membranes, *Polymer Degrad. Stab.* 94 (2009) 1955-1961.

[15] K. Yadav, K.R. Morison, Effects of hypochlorite exposure on flux through polyethersulphone ultrafiltration membranes, *Food Bioproducts Process.* 88 (2010) 419-424.

[16] B. Pellegrin, R Prulho, A. Rivaton, S. Therias, J.L. Gardette, E. Gaudichet-Maurin, C. Causserand, Hypochlorite Cleaning of Polyethersulfone/Polyvinylpyrrolidone Ultrafiltration Membranes: Impact on Performances, *Procedia Engineering* 44 (2012) 472-475.

[17] R. Prulho, A. Rivaton, S. Therias, J.L. Gardette, Ageing Mechanism of Polyethersulfone/Polyvinylpyrrolidone Membranes in Contact with Bleach Water, *Procedia Engineering* 44 (2012) 1031-1034.

- [18] R. Prulho, S. Therias, A. Rivaton, J.L. Gardette, Ageing of polyethersulfone/polyvinylpyrrolidone blends in contact with bleach water, *Polymer Degrad. Stabi.* 98 (2013) 1164-1172.
- [19] B. Pellegrin, R. Prulho, A. Rivaton, S. Therias, J.L. Gardette, E. Gaudichet-Maurin, C. Causserand, Multi-scale analysis of hypochlorite induced PES/PVP ultrafiltration membranes degradation, *J. Membr. Sci.* 447 (2013) 287-296.
- [20] C. Régula, E. Carretier, Y. Wyart, M. Sergent, G. Gésan-Guiziou, D. Ferry, A. Vincent, D. Boudot, P. Moulin, Ageing of ultrafiltration membranes in contact with sodium hypochlorite and commercial oxidant: Experimental designs as a new ageing protocol, *Sep. Purif. Technol.* 103 (2013) 119-138.
- [21] C. Regula, E. Carretier, Y. Wyart, G. Gésan-Guiziou, A. Vincent, D. Boudot, P. Moulin, Chemical cleaning/disinfection and ageing of organic UF membranes: A review, *Water Res.* 56 (2014) 325-365.
- [22] I.M. Wienk, E.E.B. Meuleman, Z Borneman, Th. van den Boomgaard, C.A. Smolders, Chemical treatment of membranes of a polymer blend: mechanism of the reaction of hypochloride with poly(vinylpyrrolidone). *J. Polym. Sci.: Part A: Polym. Chem.* 33 (1995) 49-54.
- [23] M. Rabiller-Baudry, N.W Diagne, D. Lebordais, How the experimental knowledge of the irreversible fouling distribution can contribute to understand the fluid circulation in a spiral ultrafiltration membrane, *Sep. Purif. Technol.* 136 (2014) 157-167.

Table captions

Table 1. Conditions of membrane accelerated ageing, FTIR-ATR characteristics and protein amount further adsorbed on (aged) membrane surface.

* H_{1661}^{PVP} is the height of the band located at 1661 cm^{-1} and attributed to PVP in the pristine membrane whereas H_{1240}^{PES} is the height of the band located at 1240 cm^{-1} and attributed to PES in the pristine membrane.

Table 2. Description of the 3 FTIR-ATR spectrometers used in this study

Table 3. H_i/H_{1240}^{PES} ratio from FTIR-ATR before and after fouling of pristine membrane by proteins.

Table 4. H_i/H_{1240}^{PES} ratio from FTIR-ATR before and after fouling of the 210 min micro-waves aged membrane by proteins.

Table 5. H_i/H_{1240}^{PES} ratio from FTIR-ATR before and after fouling of the 480 min micro-waves aged membrane by proteins

Table 6. Determination of $H_{1661}^{\text{protein amide I}}/H_{1240}^{PES}$ from $(H_{1539}^{\text{protein amide II}}/H_{1240}^{PES})$ for different membranes

Figure captions

Figure 1: Some polymers constituting active layer of membranes

Figure 2: Opening of the PVP ring opening by hypochlorite in alkaline conditions according to Wienk et al. [22]

Figure 3: Evolution of PES skeleton by formation of – (a) sulfonic acid group according to [14] and (b) phenol group (OH on the phenyl ring) according to [18]

Figure 4: FTIR-ATR raw spectra of a pristine PES/PVP membrane (HFK-131, Koch) in green and with smaller intensity of an industrial membrane at the end of its service life (membrane U)

Figure 5: Raw spectra of a PES/PVP membrane - (a) without or (b) with protein fouling

Figure 6: Summary of the analytical difficulty to overcome and of the proposed approach

Figure 7: NanoSIMS analysis of the pristine HFK-131 membrane highlighting presence of nitrogen. Y-axis gives the atomic ratio of organic nitrogen to sulfur considering that N comes from PVP and S from PES. The longer is the atom ablation time on the x-axis the deeper is the analysis in the membrane. There is more PVP on the surface of the membrane but it never disappears

Figure 8. Scheme of the spiral membrane with 4 double sheets highlighting the different channels in which are inserted retentate or permeate spacer, respectively. Each membrane is labelled according to the same nomenclature as those used for the quantification of protein amount for the autopsied membrane (see results). F1C1 is the innermost membrane sheet whereas F4C2 is the outermost one.

Figure 9: Evolution of flux in skim milk according to NaOCl dose received by the spiral membrane

Figure 10. Mapping of the protein irreversible deposit in the spiral membrane determined from FTIR-ATR quantification (protein amount in $\mu\text{g}\cdot\text{cm}^{-2}$) according to the location in the spiral membrane. The local TMP is calculated from the assumption of a linear pressure drop decrease. The membrane labels are defined on **Figure 8**. TMP decreases from the inlet to the outlet of the spiral membrane. d is the distance from the permeate axis ($d=0$) for a membrane sheet.

Figure 11 Mapping of $H_{1661}^{\text{raw spectrum}}/H_{1240}^{\text{PES}}$ obtained from FTIR-ATR according to the location in the spiral membrane. The local TMP is calculated from the assumption of a linear pressure drop decrease. The membrane labels are defined on **Figure 8**. TMP decreases from the inlet to the outlet of the spiral membrane. d is the distance from the permeate axis ($d=0$) for a membrane sheet.

Figure 12. Mapping of $H_{1661}^{\text{PVP}}/H_{1240}^{\text{PES}}$ obtained from **equation 3** according to the location in the spiral membrane. The local TMP is calculated from the assumption of a linear pressure drop decrease. The membrane labels are defined on **Figure 8**. TMP decreases from the inlet to the outlet of the spiral membrane. d is the distance from the permeate axis ($d=0$) for a membrane sheet

Figure 13. Mapping of $H_{1030}/H_{1240}^{\text{PES}}$ according to the location in the spiral membrane. The local TMP is calculated from the assumption of a linear pressure drop decrease. The membrane labels are defined on **Figure 8**. TMP decreases from the inlet to the outlet of the spiral membrane. d is the distance from the permeate axis ($d=0$) for a membrane sheet

APPENDICES

Appendix 1: FTIR-ATR registration

One must understand that the penetration depth of the IR incident beam in the membrane depends on the thickness of the fouling deposit. Consequently direct comparison of H_i on two spectra with different fouling amounts is not possible.

To overcome this difficulty, we pay a special attention to one of the PES membrane bands, those located at 1240 cm^{-1} (the height of which is further called H_{1240}^{PES}). This band has no overlapping with PVP and protein bands. Consequently it can be used as a reference band.

We then need to determine the $H_i/H_{1240}^{\text{PES}}$ ratio to compare variation in the quantity of the target component owing a band located at w_i .

On a practical point of view H_i has to be measured against a baseline of reference that must be chosen in a wavenumber region that is very flat and with a very small absorbance, for instance between 2240 and 2060 cm^{-1} further called $H_{2060-2240}^{\text{baseline}}$ with spectrometer 1.

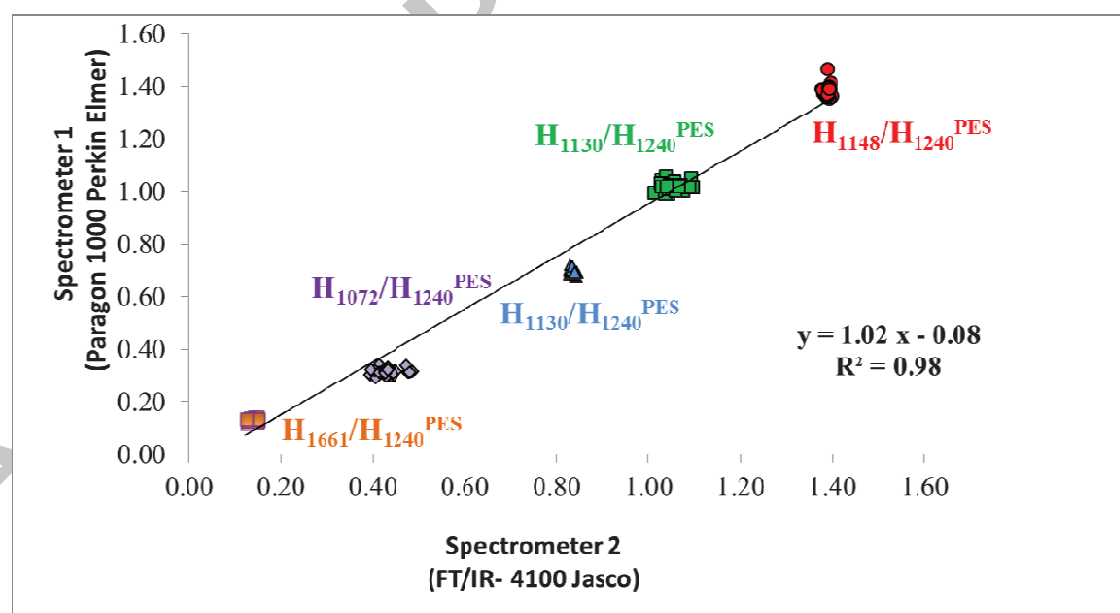
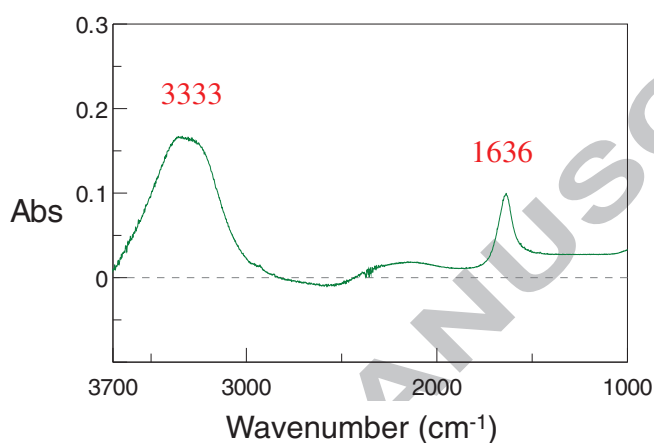


Figure A1-1 : Linear relationship between band height ratio ($H_i/H_{1240}^{\text{PES}}$) measured on different pristine HFK-131 membranes with spectrometer 1 and spectrometer 2. Similar results are obtained when comparing spectrometer 1 and spectrometer 3.

Appendix 2: Determination of γ for FTIR-ATR analysis of proteins in aqueous solutions.

The spectrum of water is firstly registered (**Figure A2-1 a**): two main bands due to OH bond are observed located close to 3333 cm^{-1} and 1636 cm^{-1} , respectively.

(a)



(b)

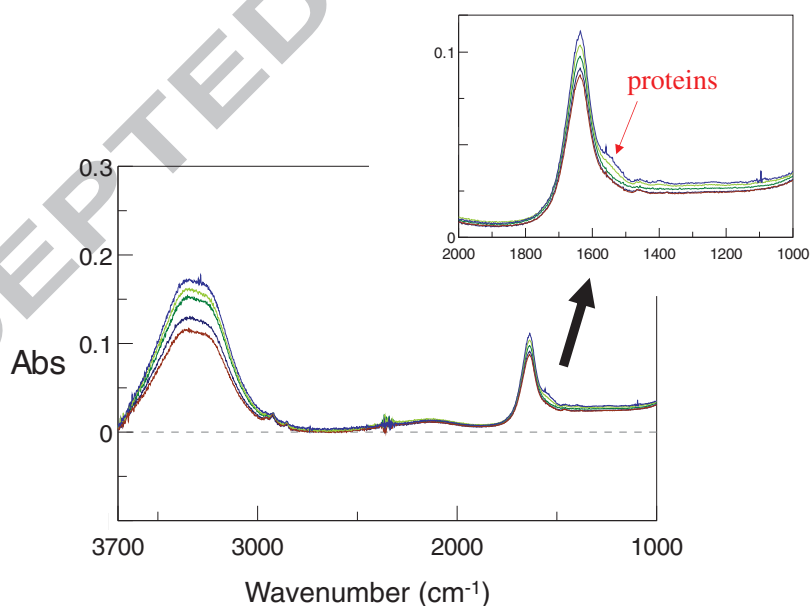


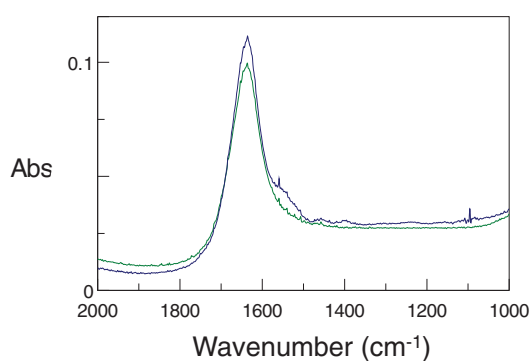
Figure A2-1: FTIR-ATR raw spectra- (a) water – (b) protein solutions in water

The spectra of protein solutions (protein concentration between $5\text{ g}\cdot\text{L}^{-1}$ and $50\text{ g}\cdot\text{L}^{-1}$) are registered (**Figure A2-1 b**). At first sight bands of water are easily observed. Looking carefully close to

1500-1600 cm^{-1} , it is shown that shoulders appear in the 1636 cm^{-1} band of water. These shoulder correspond to amide I and amide II band of proteins, as it can be evidenced after substraction according to **equation A2-1** (**Figure A2-2b**).

$$\text{Protein difference spectrum} = \text{Protein raw spectrum} - \text{water spectrum} \quad (\text{eq. A2-1})$$

(a)



(b)

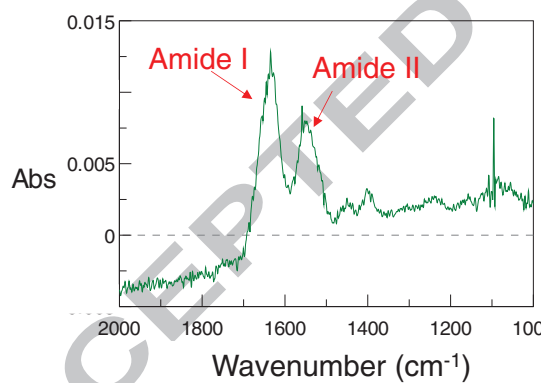
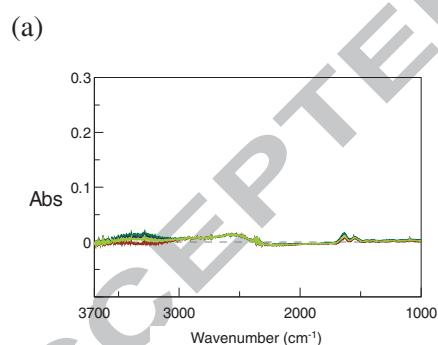


Figure A1-2: FTIR-ATR spectra in the 2000-1000 cm^{-1} region. (a) raw spectra of water and protein solution at 50 g.L^{-1} – (b) difference spectrum obtained according to **equation A2-1**.

The use of **equation A2-1** is correct as a first estimation and for qualitative purpose. But in order to have a better accuracy on the height of protein bands for quantitative purpose, the equation must be modified by introducing a corrective term, further called γ leading at least to **equation A2-2** (similar to **eq. 6** in the full paper).

$$\text{Protein difference spectrum} = \text{Protein raw spectrum} - \gamma \text{water spectrum} \quad (\text{eq. A2-2})$$

The value of γ is determined from the simultaneous cancellation of both the 3333 and 1636 cm^{-1} bands of the raw spectra attributed to water. **Figure A2-3** illustrates the impact of γ choice that is adjusted up to obtain a difference spectrum as flat as possible in the regions of interest.



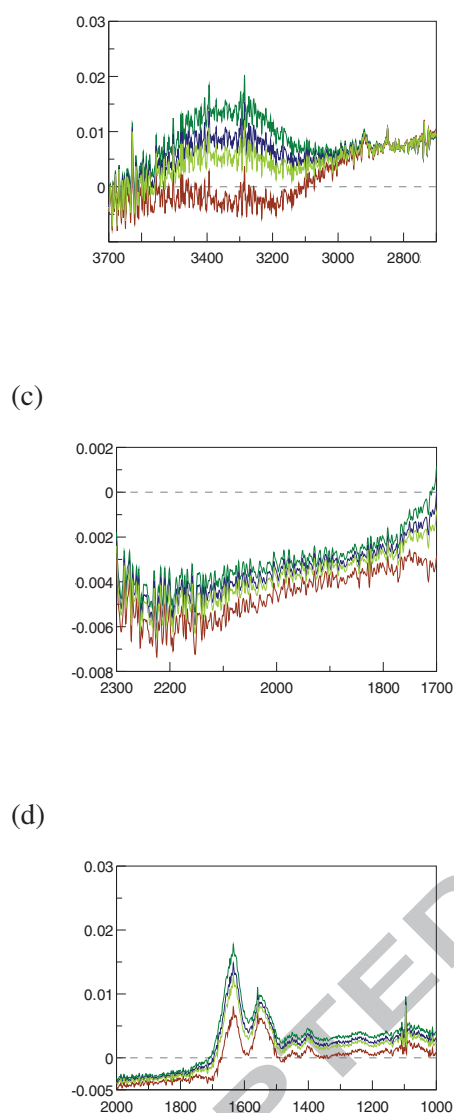


Figure A2-3: FTIR-ATR difference spectra obtained from protein solution spectrum (50 g.L^{-1}) and water spectrum according to **equation A2** with various γ value in the range 0.95 – 1.05- (a) 3700-1000 cm^{-1} range- (b) zoom in the 3700-2800 cm^{-1} region to evidence cancellation of the 3333 cm^{-1} water band –(c) zoom in the 2300-1700 cm^{-1} region and (d) zoom in the 2000-1000 cm^{-1} region to evidence cancellation of the 1661 cm^{-1} water band and the appearance of amide I and amide II protein bands.

Such determination have been done for the different protein concentration. **Table A2-1** shows the optimized γ values for spectrum used in this study.

Table A2-1. Optimised γ value for difference spectrum (according to **equation A2**) for each protein solution. :

Protein concentration (g.L ⁻¹)	γ
5	0.920
10	0.800
20	0.699
30	0.780
50	1.018

Appendix 3: Attempt of correlation between PVP and PES degradation

The aim is to evidence possible correlation between the disappearance of PVP and the degradation of PES (**Figure A3-1**). None is found.

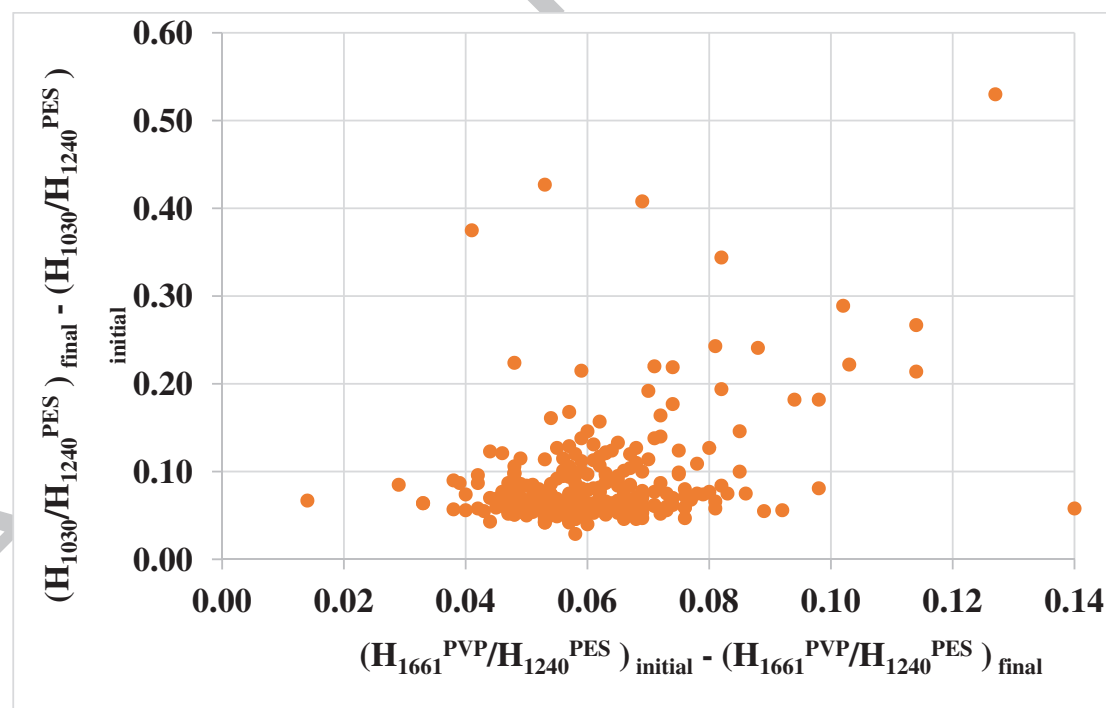


Figure A3-1: Increase of 1030cm^{-1} band (according to FTIR-ATR, pristine membrane value is 0.04) versus decrease of PVP (according to FTIR-ATR, pristine membrane value is 0.14) - (spectra acquired on 334 samples of CIP-3 spiral membrane)

Appendix 4: FTIR-ATR supporting data corresponding to Figures 10 (A4-1), 11 (A4-2), 12 (A4-3), 13 (A4-4).

	F1C1				F1C2			
	Inlet		Outlet		Inlet		Outlet	
	TMP(bar)				TMP(bar)			
	5.0	4.5	3.9	3.4	5.0	4.5	3.9	3.4
d (mm)	permeate axis							
45	68	71	57	55	59	54	57	64
135	60	58	54	49	57	59	53	51
225	58	56	58	53	54	58	53	52
315	54	61	53	49	49	43	50	52
405	52	51	53	49	48	46	50	47
495	53	52	51	48	50	57	48	44
585	51	50	49	53	62	46	42	47
675	49	55	49	46	42	52	48	61
765	47	49	48	46	47	43	42	33
855	51	48	58	47	57	34	42	38
945	37	37	42	39	25	25	26	26

F2C1					F2C2						
	Inlet		Outlet				Inlet		Outlet		
	TMP(bar)					TMP(bar)					
	5.0	4.5	3.9	3.4		5.0	4.5	3.9	3.4		
d (mm)	permeate axis					permeate axis					
45	75	64	65	53		74	73	52	55		
135	49	74	53	43		68	54	55	49		
225	69	56	40	46		61	62	55	56		
315	55	55	39	46		53	60		47		
405	46	54	47	43		54	53	50	47		
495	56	48	43	47		53	49	48	46		
585	44	53	50	44		50	52	48	50		
675	54	50	48	46		51	50	46	42		
765	45	42	41	42		47	48	42	40		
855											
945											

F3C1					F3C2						
	Inlet		Outlet				Inlet		Outlet		
	TMP(bar)					TMP(bar)					
	5.0	4.5	3.9	3.4		5.0	4.5	3.9	3.4		
d (mm)	permeate axis					permeate axis					
45	82	60	58	56		63	58	51	54		
135	58	56	60	52		68	53	64	50		
225	69	56	52	48		41	63	58	55		
315	56	53	46	44		61	56	59	53		
405	52	62	46	47		54	53	49	35		
495	50	52	47	48		49	70	61	50		
585	49	44	47	44		54	57	51	48		
675	45	49	49	48		56	51	55	36		
765	45	41	44	42		49	49	50	38		
855	39	41	46	44		58	41	40	42		
945						13	40	40	29		

F4C1					F4C2						
	Inlet		Outlet				Inlet		Outlet		
	TMP(bar)					TMP(bar)					
	5.0	4.5	3.9	3.4		5.0	4.5	3.9	3.4		
d (mm)	permeate axis					permeate axis					
45	71	54	61	54		73	66	52	50		
135	62	62	66	49		59	65	51	48		
225	57	60	64	48		63	41	46	49		
315	53	48	61	47		48	47	44	50		
405	53	51	53	45		43	54	70	46		
495	47	51	53	48		46	49	45	35		
585	49	51	50	51		40	45	46	42		
675	47	52	48	45		49	43	49	37		
765	49	40	48	46		48	36	73	31		
855	46	45	42	37		47	44	44	32		
945											

Figure A4-1. Mapping of the protein irreversible deposit in the spiral membrane determined from FTIR-ATR quantification (protein amount in $\mu\text{g}\cdot\text{cm}^{-2}$) according to the location in the spiral membrane. The local TMP is calculated from the assumption of a linear pressure drop decrease. The membrane labels are defined on **Figure 8**. (white = not determined)

d (mm)	F1C1				F1C2			
	Inlet		Outlet		Inlet		Outlet	
	TMP(bar)				TMP(bar)			
	5.0	4.5	3.9	3.4	5.0	4.5	3.9	3.4
	permeate axis				permeate axis			
45	0.306	0.316	0.268	0.257	0.283	0.272	0.242	0.261
135	0.269	0.274	0.252	0.248	0.283	0.280	0.263	0.258
225	0.276	0.267	0.274	0.251	0.268	0.279	0.268	0.244
315	0.248	0.259	0.255	0.235	0.235	0.222	0.257	0.230
405	0.251	0.249	0.260	0.239	0.237	0.221	0.254	0.244
495	0.261	0.256	0.255	0.232	0.236	0.255	0.245	0.226
585	0.242	0.250	0.242	0.248	0.234	0.242	0.206	0.241
675	0.240	0.250	0.239	0.235	0.194	0.254	0.238	0.221
765	0.236	0.243	0.242	0.233	0.215	0.219	0.237	0.173
855	0.253	0.237	0.258	0.234	0.117	0.205	0.218	0.196
945	0.197	0.202	0.219	0.194	0.139	0.150	0.158	0.150

F2C1					F2C2				
d (mm)	Inlet		Outlet		Inlet		Outlet		
	TMP(bar)				TMP(bar)				
	5.0	4.5	3.9	3.4	5.0	4.5	3.9	3.4	
	permeate axis				permeate axis				
45	0.333	0.297	0.289	0.253	0.303	0.289	0.248	0.250	
135	0.250	0.336	0.260	0.228	0.295	0.266	0.263	0.252	
225	0.264	0.267	0.215	0.234	0.287	0.281	0.252	0.248	
315	0.257	0.251	0.204	0.214	0.255	0.286	?	0.239	
405	0.233	0.259	0.240	0.221	0.260	0.254	0.248	0.240	
495	0.256	0.232	0.222	0.228	0.264	0.252	0.245	0.239	
585	0.221	0.256	0.237	0.211	0.255	0.195	0.247	0.240	
675	0.255	0.249	0.239	0.233	0.259	0.255	0.243	0.223	
765	0.220	0.214	0.217	0.214	0.242	0.244	0.222	0.206	
855									
945									

F3C1					F3C2				
d (mm)	Inlet		Outlet		Inlet		Outlet		
	TMP(bar)				TMP(bar)				
	5.0	4.5	3.9	3.4	5.0	4.5	3.9	3.4	
	permeate axis				permeate axis				
45	0.335	0.302	0.261	0.270	0.272	0.270	0.240	0.267	
135	0.275	0.271	0.279	0.248	0.309	0.274	0.272	0.255	
225	0.285	0.275	0.268	0.248	0.262	0.281	0.280	0.261	
315	0.262	0.259	0.233	0.243	0.271	0.267	0.262	0.246	
405	0.257	0.268	0.235	0.231	0.259	0.269	0.247	0.230	
495	0.246	0.263	0.242	0.240	0.259	0.288	0.265	0.253	
585	0.243	0.231	0.244	0.233	0.256	0.257	0.259	0.248	
675	0.233	0.235	0.245		0.251	0.250	0.261	0.223	
765	0.256	0.221	0.228	0.222	0.242	0.247	0.254	0.227	
855	0.218	0.220	0.234	0.229	0.271	0.227	0.235	0.220	
945					0.138	0.205	0.217	0.172	

F4C1					F4C2				
d (mm)	Inlet		Outlet		Inlet		Outlet		
	TMP(bar)				TMP(bar)				
	5.0	4.5	3.9	3.4	5.0	4.5	3.9	3.4	
	permeate axis				permeate axis				
45	0.316	0.265	0.283	0.239	0.274	0.290	0.255	0.251	
135	0.275	0.278	0.264	0.246	0.275	0.251	0.204	0.235	
225	0.266	0.273	0.297	0.239	0.289	0.213	0.235	0.251	
315	0.255	0.235	0.274	0.228	0.248	0.237	0.212	0.231	
405	0.257	0.257	0.240	0.231	0.213	0.266	0.272	0.221	
495	0.244	0.253	0.265	0.234	0.230	0.217	0.216	0.189	
585	0.243	0.240	0.244	0.228	0.211	0.225	0.227	?	
675	0.232	0.249	0.220	0.215	0.229	0.225	0.232	0.186	
765	0.256	0.206	0.231	0.243	0.250	0.205	0.244	0.192	
855	0.227	0.225	0.199	0.191	0.220	0.201	0.226	0.176	
945									

Figure A4-2 Mapping of $H_{1661}^{\text{raw spectra}}/H_{1240}^{\text{PES}}$ obtained from FTIR-ATR according to the location in the spiral membrane. The local TMP is calculated from the assumption of a linear pressure drop decrease. The membrane labels are defined on **Figure 8**. (white = not determined)

F1C1					F1C2				
	Inlet					Outlet			
	TMP(bar)					TMP(bar)			
	5.0	4.5	3.9	3.4		5.0	4.5	3.9	3.4
d (mm)	permeate axis					permeate axis			
45	0.090	0.091	0.085	0.079		0.092	0.098	0.059	0.058
135	0.078	0.089	0.077	0.086		0.099	0.089	0.091	0.092
225	0.089	0.085	0.086	0.078		0.093	0.092	0.094	0.073
315	0.073	0.063	0.082	0.075		0.074	0.079	0.095	0.062
405	0.069	0.048	0.075	0.078		0.081	0.069	0.092	0.090
495	0.088	0.086	0.088	0.075		0.072	0.071	0.089	0.080
585	0.078	0.087	0.082	0.076		0.037	0.085	0.067	0.087
675	0.080	0.073	0.079	0.082		0.055	0.086	0.081	0.026
765	0.081	0.083	0.084	0.081		0.060	0.077	0.096	0.060
855	0.088	0.079	0.072	0.080		0	0.088	0.077	0.069
945	0.071	0.077	0.080	0.064		0.051	0.059	0.064	0.058

F2C1					F2C2				
	Inlet					Outlet			
	TMP(bar)					TMP(bar)			
	5.0	4.5	3.9	3.4		5.0	4.5	3.9	3.4
d (mm)	permeate axis					permeate axis			
45	0.096	0.093	0.081	0.082		0.068	0.058	0.079	0.073
135	0.091	0.102	0.087	0.087		0.078	0.089	0.086	0.092
225	0.046	0.086	0.081	0.082		0.092	0.083	0.074	0.067
315	0.079	0.073	0.072	0.061		0.083	0.092		0.085
405	0.083	0.083	0.087	0.079		0.085	0.081	0.085	0.084
495	0.076	0.074	0.081	0.072		0.091	0.091	0.087	0.086
585	0.075	0.084	0.074	0.066		0.091	0.026	0.089	0.077
675	0.081	0.086	0.083	0.082		0.092	0.091	0.090	0.084
765	0.072	0.072	0.079	0.074		0.086	0.087	0.081	0.073
855									
945									

F3C1					F3C2				
	Inlet					Outlet			
	TMP(bar)					TMP(bar)			
	5.0	4.5	3.9	3.4		5.0	4.5	3.9	3.4
d (mm)	permeate axis					permeate axis			
45	0.077	0.107	0.075	0.090		0.070	0.082	0.073	0.092
135	0.089	0.088	0.086	0.078		0.094	0.101	0.068	0.093
225	0.066	0.095	0.097	0.090		0.126	0.081	0.094	0.083
315	0.082	0.088	0.080	0.096		0.076	0.086	0.072	0.075
405	0.087	0.071	0.084	0.078		0.085	0.098	0.087	0.111
495	0.082	0.093	0.086	0.083		0.098	0.065	0.071	0.089
585	0.083	0.086	0.090	0.087		0.082	0.072	0.093	0.092
675	0.085	0.075	0.084			0.071	0.083	0.082	0.100
765	0.107	0.085	0.083	0.081		0.081	0.086	0.091	0.100
855	0.087	0.083	0.082	0.083		0.085	0.089	0.102	0.079
945						0.082	0.071	0.082	0.069

F4C1					F4C2				
	Inlet					Outlet			
	TMP(bar)					TMP(bar)			
	5.0	4.5	3.9	3.4		5.0	4.5	3.9	3.4
d (mm)	permeate axis					permeate axis			
45	0.092	0.088	0.089	0.064		0.042	0.080	0.086	0.086
135	0.081	0.055	0.087	0.081		0.086	0.042	0.038	0.078
225	0.082	0.092	0.083	0.083		0.087	0.075	0.082	0.090
315	0.077	0.078	0.073	0.084		0.090	0.081	0.065	0.068
405	0.090	0.069	0.083	0.090		0.071	0.092	0.052	0.070
495	0.087	0.092	0.075	0.084		0.080	0.057	0.066	0.069
585	0.074	0.080	0.062	0.078		0.078	0.077	0.075	
675	0.080	0.064	0.066	0.094		0.068	0.081	0.071	0.060
765	0.071	0.074	0.091	0.077		0.092	0.083	0.013	0.085
855	0.077	0.059	0.065	0.077		0.067	0.054	0.080	0.064
945									

Figure A4-3. Mapping of $H_{1661}^{PVP}/H_{1240}^{PES}$ obtained from **equation 3** according to the location in the spiral membrane. The local TMP is calculated from the assumption of a linear pressure drop decrease. The membrane labels are defined on **Figure 8**. (white = not determined)

ACCEPTED MANUSCRIPT

F1 C1					F1 C2				
d (mm)	Inlet		Outlet		Inlet		Outlet		
	TMP (bar)				TMP (bar)				
	5.0	4.5	3.9	3.4	5.0	4.5	3.9	3.4	
	permeate axis				permeate axis				
45	0.124	0.126	0.108	0.121	0.264	0.136	0.283	0.234	
135	0.110	0.112	0.106	0.092	0.415	0.125	0.155	0.117	
225	0.111	0.105	0.114	0.118	0.127	0.138	0.113	0.144	
315	0.103	0.108	0.109	0.096	0.141	0.171	0.099	0.149	
405	0.101	0.096	0.100	0.100	0.121	0.178	0.098	0.092	
495	0.101	0.103	0.099	0.107	0.167	0.448	0.094	0.119	
585	0.096	0.098	0.116	0.097	0.262	0.132	0.115	0.088	
675	0.103	0.097	0.100	0.088	0.140	0.104	0.255	0.307	
765	0.099	0.108	0.101	0.109	0.167	0.162	0.110	0.117	
855	0.104	0.104	0.102	0.104	0.098	0.120	0.093	0.117	
945	0.087	0.091	0.092	0.112	0.095	0.098	0.087	0.124	

F2 C1					F2 C2				
d (mm)	Inlet		Outlet		Inlet		Outlet		
	TMP (bar)				TMP (bar)				
	5.0	4.5	3.9	3.4	5.0	4.5	3.9	3.4	
	permeate axis				permeate axis				
45	0.163	0.119	0.178	0.127	0.204	0.384	0.153	0.124	
135	0.124	0.130	0.104	0.084	0.122	0.120	0.114	0.096	
225	0.222	0.094	0.152	0.096	0.116	0.114	0.121	0.100	
315	0.100	0.096	0.098	0.114	0.144	0.111		0.091	
405	0.091	0.134	0.089	0.098	0.100	0.119	0.098	0.105	
495	0.104	0.115	0.091	0.086	0.100	0.094	0.091	0.110	
585	0.124	0.135	0.091	0.110	0.100	0.254	0.101	0.161	
675	0.099	0.091	0.105	0.086	0.095	0.098	0.095	0.098	
765	0.098	0.111	0.093	0.086	0.108	0.099	0.097	0.092	
855									
945									

F3 C1					F3 C2				
d (mm)	Inlet		Outlet		Inlet		Outlet		
	TMP (bar)				TMP (bar)				
	5.0	4.5	3.9	3.4	5.0	4.5	3.9	3.4	
	permeate axis				permeate axis				
45	0.127	0.104	0.135	0.106	0.232	0.136	0.125	0.146	
135	0.096	0.106	0.099	0.117	0.117	0.127	0.127	0.105	
225	0.217	0.109	0.095	0.098	0.107	0.141	0.101	0.115	
315	0.111	0.099	0.080	0.083	0.164	0.201	0.150	0.098	
405	0.114	0.103	0.101	0.102	0.109	0.127	0.116	0.125	
495	0.092	0.092	0.090	0.091	0.098	0.137	0.112	0.098	
585	0.094	0.095	0.090	0.087	0.098	0.148	0.094	0.091	
675	0.090	0.098	0.093	0.096	0.110	0.208	0.119	0.096	
765	0.104	0.089	0.085	0.094	0.107	0.109	0.094	0.114	
855	0.082	0.082	0.090	0.084	0.101	0.105	0.097	0.097	
945					0.069	0.118	0.086	0.102	

F4 C1					F4 C2				
d (mm)	Inlet		Outlet		Inlet		Outlet		
	TMP (bar)				TMP (bar)				
	5.0	4.5	3.9	3.4	5.0	4.5	3.9	3.4	
	permeate axis				permeate axis				
45	0.131	0.116	0.122	0.120	0.222	0.137	0.110	0.111	
135	0.140	0.186	0.467	0.097	0.126	0.121	0.329	0.157	
225	0.160	0.137	0.169	0.101	0.154	0.173	0.103	0.099	
315	0.128	0.147	0.160	0.141	0.102	0.101	0.164	0.180	
405	0.106	0.101	0.146	0.096	0.096	0.139	0.281	0.154	
495	0.082	0.110	0.093	0.155	0.186	0.115	0.102	0.260	
585	0.102	0.119	0.115	0.197	0.116	0.136	0.130		
675	0.103	0.099	0.259	0.161	0.092	0.119	0.140	0.116	
765	0.093	0.096	0.111	0.092	0.091	0.083	0.570	0.167	
855	0.098	0.106	0.139	0.138	0.096	0.115	0.096	0.099	
945									

Figure A4-4. Mapping of H_{1030}/H_{1240}^{PES} according to the location in the spiral membrane. The local TMP is calculated from the assumption of a linear pressure drop decrease. The membrane labels are defined on **Figure 8**. (white = not determined).

Tables

Table 1. Conditions of membrane accelerated ageing, FTIR-ATR characteristics and protein amount further adsorbed on (aged) membrane surface.

	Ageing time (min) (micro-waves)	FTIR-ATR* $H_{1661}^{PVP}/H_{1240}^{PES}$	Range of protein deposit on membrane surface ($\mu\text{g}\cdot\text{cm}^{-2}$)
Pristine membrane	0	0.14 ± 0.01 (n=6)	0 – 208
Ageing by NaOCl	210	0.10 ± 0.01 (n=6)	0 - 76
Ageing by NaOCl	480	0.07 ± 0.01 (n=6)	0- 82

* H_{1661}^{PVP} is the height of the band located at 1661 cm^{-1} and attributed to PVP in the pristine membrane whereas H_{1240}^{PES} is the height of the band located at 1240 cm^{-1} and attributed to PES in the pristine membrane.

Table 2. Description of the three FTIR-ATR spectrometers used in this study

	Spectrometer 1	Spectrometer 2	Spectrometer 3
	Paragon 1000	FT/IR-4100	Spectrum 100
	Perkin-Elmer	Jasco	Perkin Elmer
ATR	ZnSe crystal	ZnSe crystal	Diamond crystal
accessory	incidence angle: 45°	incidence angle: 45°	incidence angle: 45°
	12 reflections	1 reflection	1 reflection
Crystal dimension	2 cm x 5 cm	1.8 mm diameter	2 mm diameter
Software	Spectrum for windows 5	Spectra Manager II	Spectrum for windows 6
Acquisition conditions	spectral domain : 4000-600 cm ⁻¹	spectral domain : 3700-600 cm ⁻¹	spectral domain : 4000-600 cm ⁻¹
	resolution : 2 cm ⁻¹	resolution : 2 cm ⁻¹	resolution : 2 cm ⁻¹
	20 scans	128 scans	20 scans
	background : air	background : air	background : air

Table 3. $H_{1661}^{PES}/H_{1240}^{PES}$ ratio from FTIR-ATR before and after fouling of pristine membrane by proteins.

Protein concentration in solution (g.L ⁻¹)	$H_{1661}^{PVP}/H_{1240}^{PES}$ (pristine)	$H_{1661}^{raw\ spectra}/H_{1240}^{PES}$ (fouled)	$H_{1539}^{protein\ amide\ II}/H_{1240}^{PES}$ (fouled)	$H_{1661}^{protein\ amide\ I}/H_{1240}^{PES}$ (from Eq. 3)
0	0.152			
5	0.137	0.202	0.084	0.065
10	0.125	0.264	0.150	0.139
20	0.148	0.321	0.197	0.174
30	0.146	0.633	0.568	0.487
50	0.134	0.742	0.723	0.608

Table 4– H_i/H_{1240}^{PES} ratio from FTIR-ATR before and after fouling of the 210 min micro-waves aged membrane by proteins.

Protein concentration in solution (g.L ⁻¹)	$H_{1661}^{PVP}/H_{1240}^{PES}$ (not fouled)	$H_{1661}^{raw\ spectra}/H_{1240}^{PES}$ (fouled)	$H_{1539}^{protein\ amide}/H_{1240}^{PES}$ (fouled)	$H_{1661}^{protein\ amide}/H_{1240}^{PES}$ (from Eq. 3)
0	0.116			
5	0.084	0.149	0.084	0.065
10	0.093	0.167	0.094	0.075
20	0.093	0.198	0.126	0.105
30	0.100	0.290	0.213	0.189
50	0.099	0.348	0.275	0.248

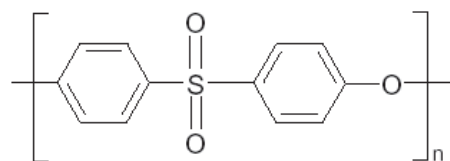
Table 5 – H_i/H_{1240}^{PES} ratio from FTIR-ATR before and after fouling of the 480 min micro-waves aged membrane by proteins

Protein concentration in solution (g.L ⁻¹)	$H_{1661}^{PVP}/H_{1240}^{PES}$ (not fouled)	$H_{1661}^{raw\ spectra}/H_{1240}^{PES}$ (fouled)	$H_{1539}^{protein\ amide}/H_{1240}^{PES}$ (fouled)	$H_{1661}^{protein\ amide}/H_{1240}^{PES}$ (from Eq. 3)
0	0.073			
5	0.058	0.113	0.060	0.055
10	0.060	0.154	0.098	0.094
20	0.066	0.208	0.144	0.141
30	0.076	0.252	0.177	0.176
50	0.062	0.361	0.297	0.299

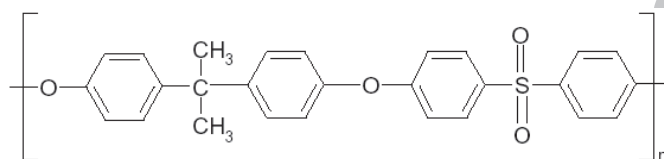
Table 6- Determination of $H_{1661}^{\text{protein amide I}}/H_{1240}^{\text{PES}}$ from $(H_{1539}^{\text{protein amide II}}/H_{1240}^{\text{PES}})$ for different membranes

$(H_{1661}^{\text{PVP}}/H_{1240}^{\text{PES}})$	$H_{1661}^{\text{protein amide I}}/H_{1240}^{\text{PES}} = a$ $(H_{1539}^{\text{protein amide II}}/H_{1240}^{\text{PES}}) (y = a x)$	Number of values	Correlation coefficient R^2	Range of protein amount on membrane surface ($\mu\text{g}\cdot\text{cm}^{-2}$)
0.14 (Pristine)	$y = 0.85 x$	6	0.999	0 - 208
0.10 (210 min aged)	$y = 0.88 x$	6	0.975	0 - 76
0.07 (480 min aged)	$y = 0.99 x$	6	0.996	0 - 82
Average	$y = 0.87 x$	18	0.991	0 - 76 (208)

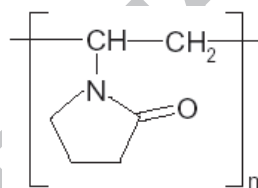
Figures



(a) Polyethersulfone



(b) Polysulfone



(c) Polyvinylpyrrolidone

Figure 1: Some polymers constituting active layer of membranes

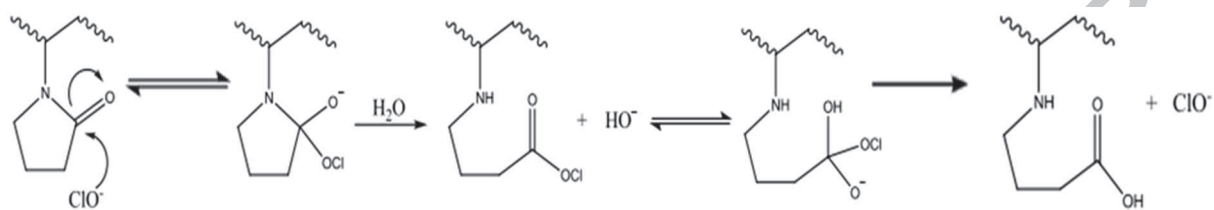
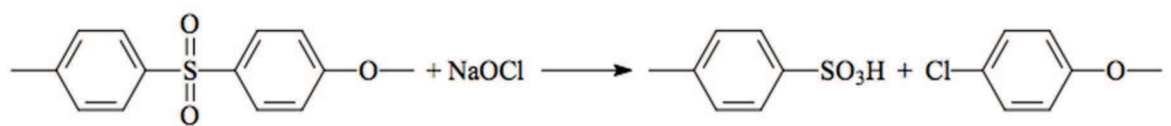
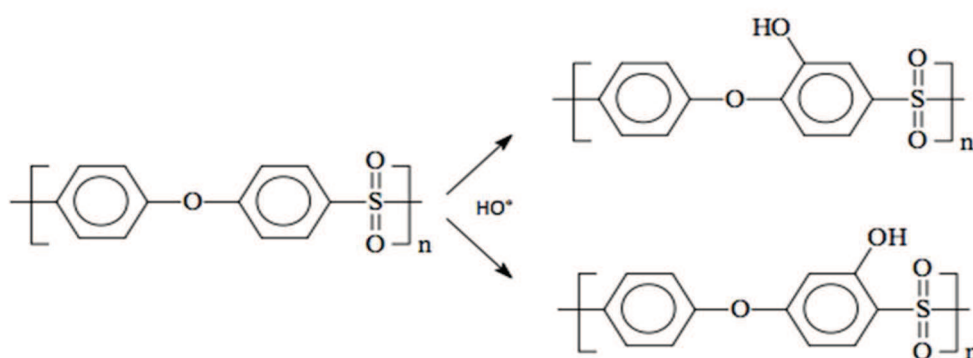


Figure 2: Opening of the PVP ring opening by hypochlorite in alkaline conditions according to Wienk et al. [22]



(a)



(b)

Figure 3: Evolution of PES skeleton by formation of – (a) sulfonic acid group according to [14] and (b) phenol group (OH on the phenyl ring) according to [18]

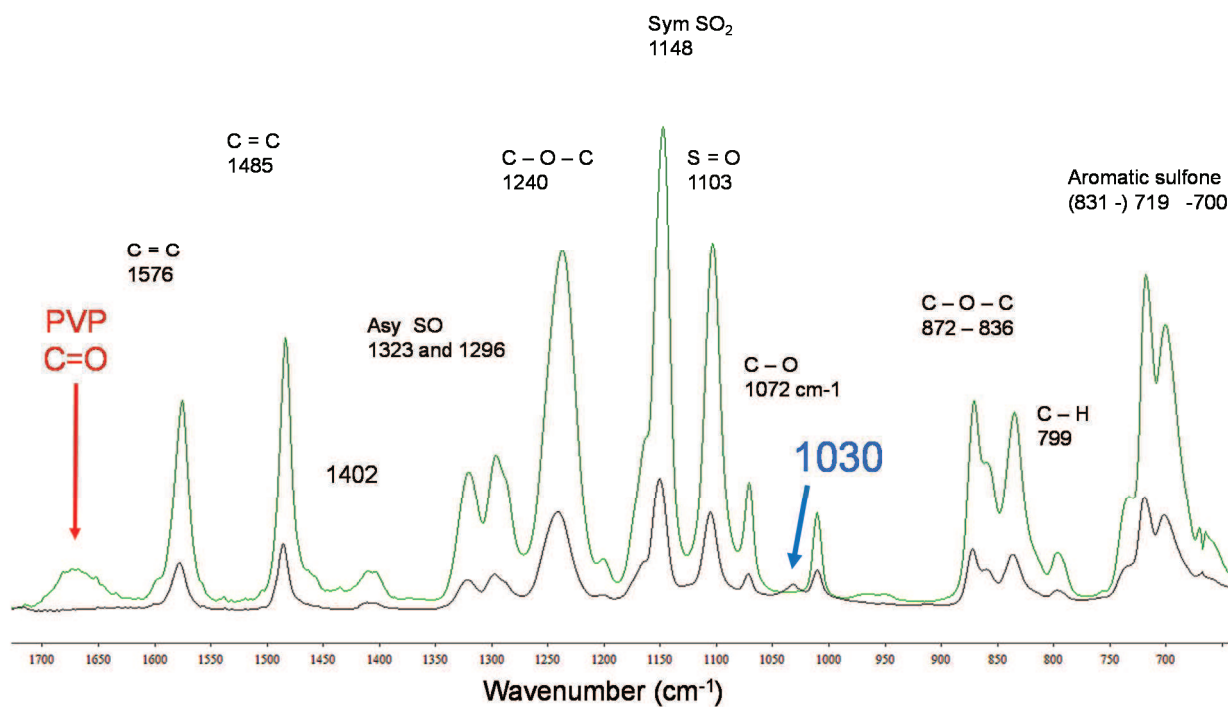


Figure 4: FTIR-ATR raw spectra of a pristine PES/PVP membrane (HFK-131, Koch) in green and with smaller intensity of an industrial membrane at the end of its service life (membrane U)

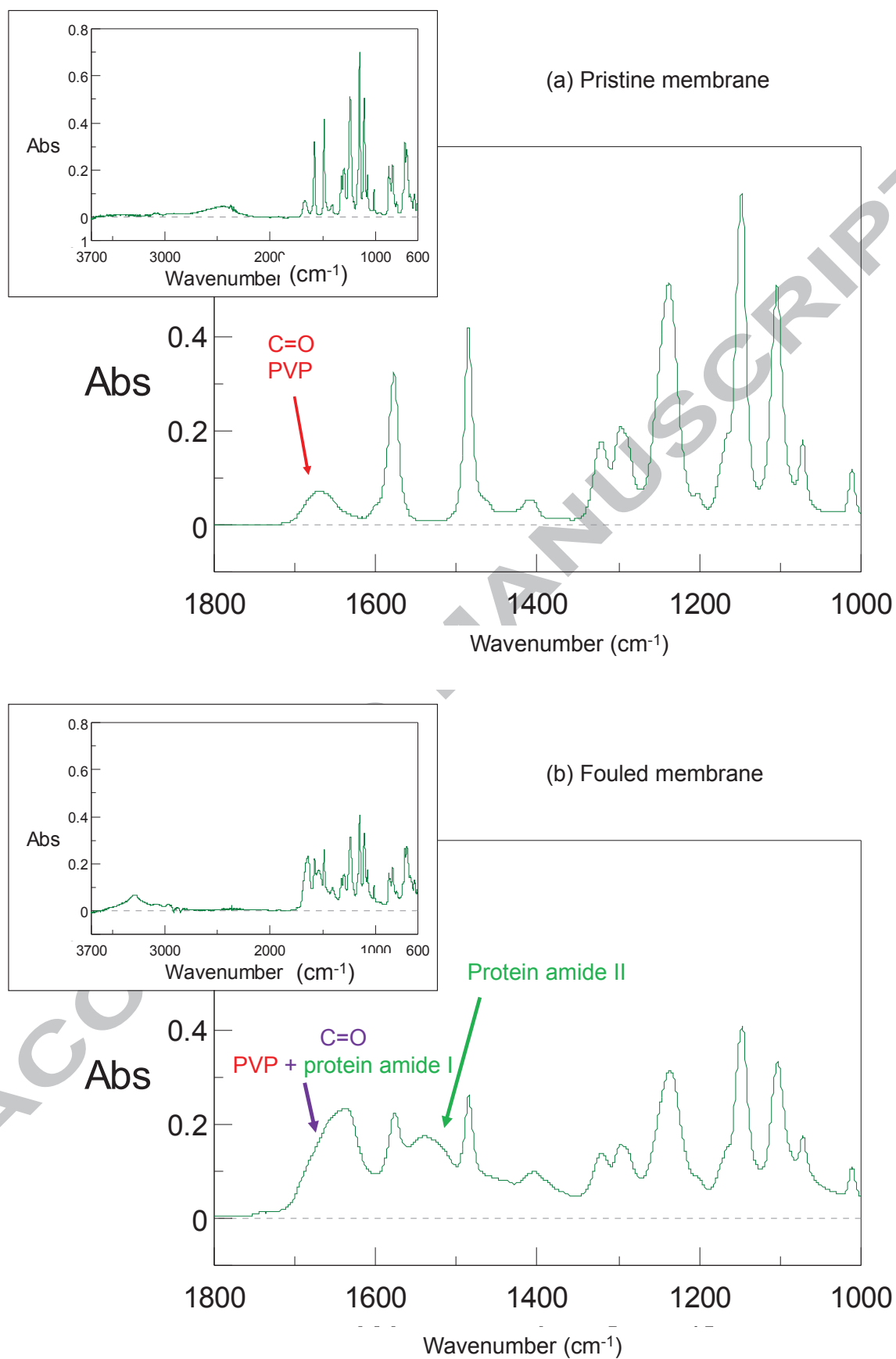


Figure 5: Raw spectra of a PES/PVP membrane - (a) without or (b) with protein fouling

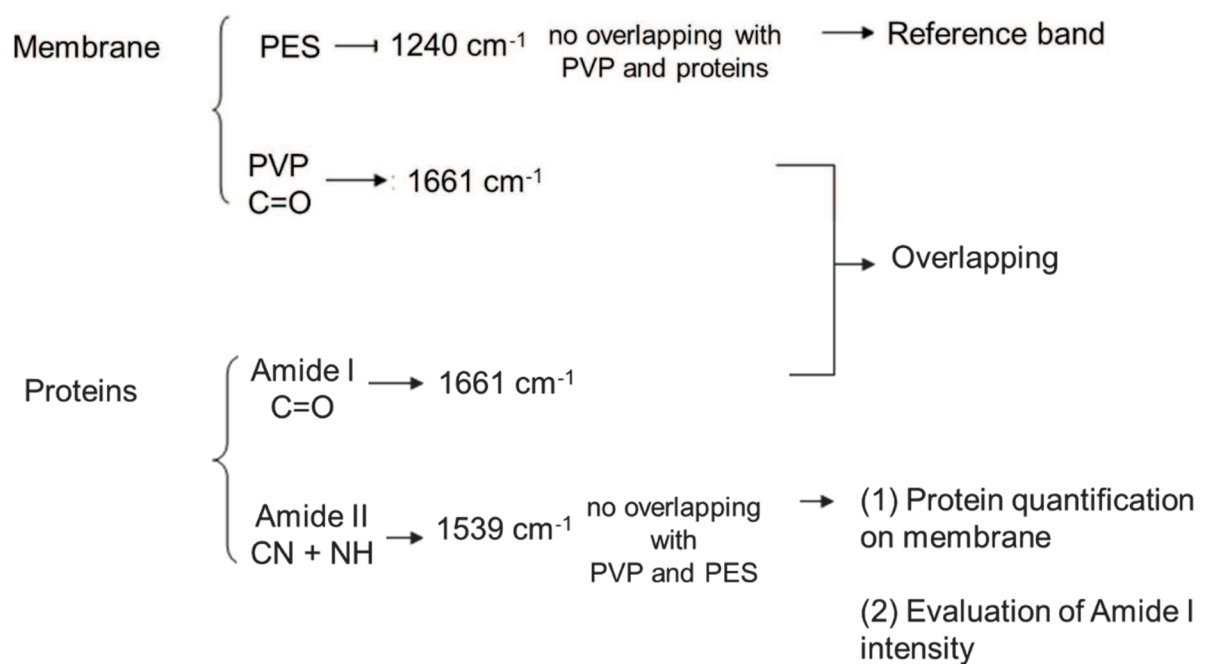


Figure 6: Summary of the analytical difficulty to overcome and of the proposed approach

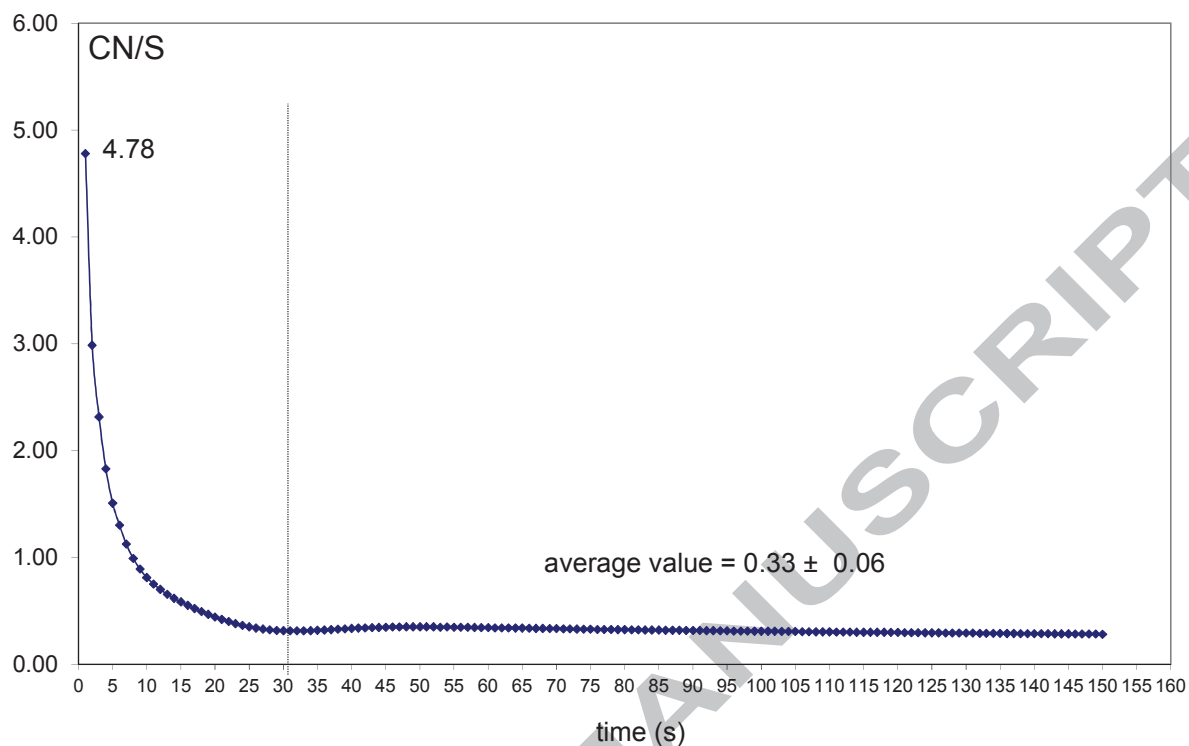


Figure 7: NanoSIMS analysis of the pristine HFK-131 membrane highlighting presence of nitrogen. Y-axis gives the atomic ratio of organic nitrogen to sulfur considering that N comes from PVP and S from PES. The longer is the atom ablation time on the x-axis the deeper is the analysis in the membrane. There is more PVP on the surface of the membrane but it never disappears

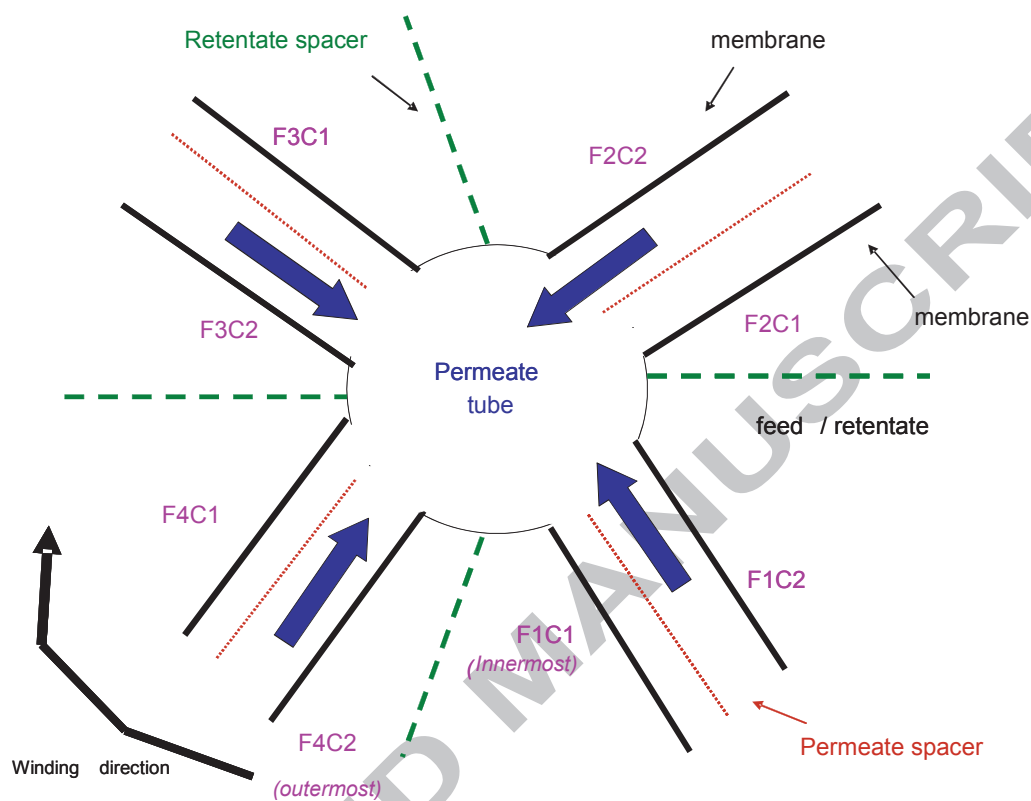


Figure 8. Scheme of the spiral membrane with 4 double sheets highlighting the different channels in which are inserted retentate or permeate spacer, respectively. Each membrane is labelled according to the same nomenclature as those used for the quantification of protein amount for the autopsied membrane (see results). F1C1 is the innermost membrane sheet whereas F4C2 is the outermost one.

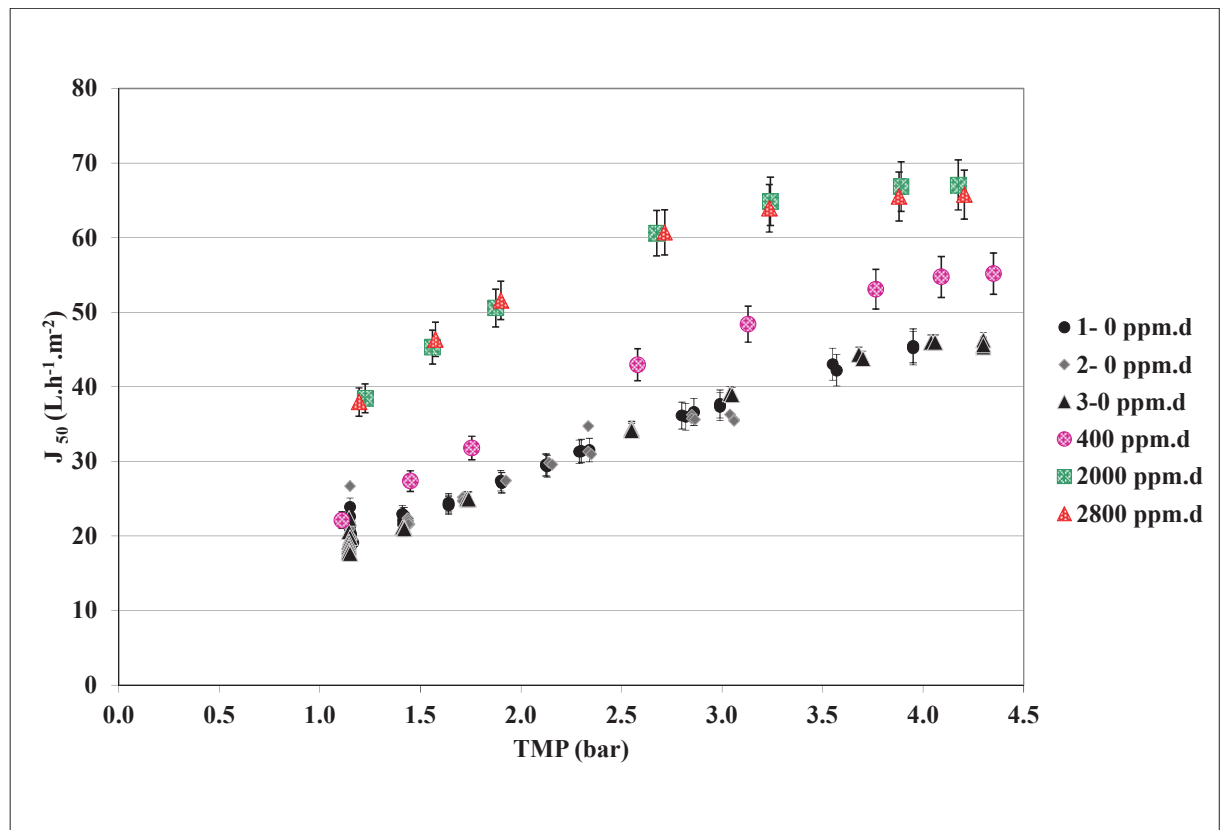
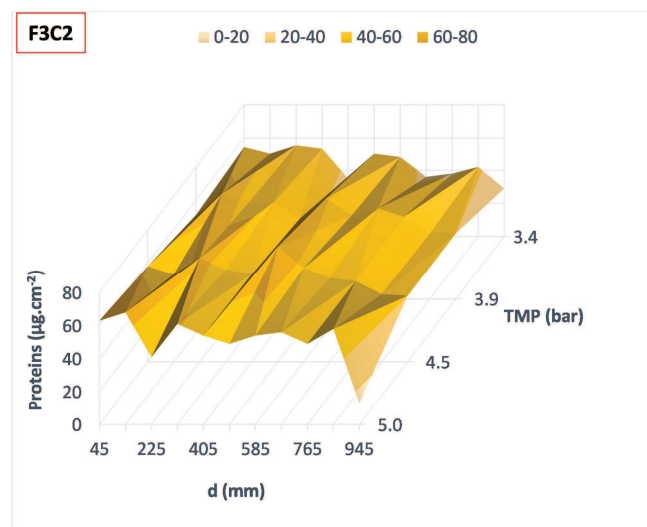
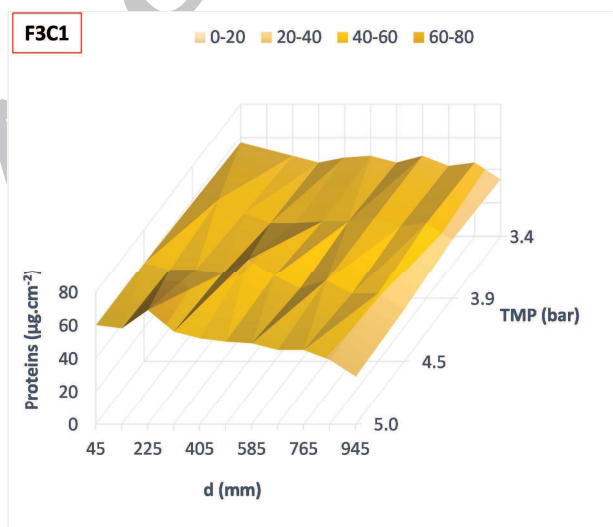
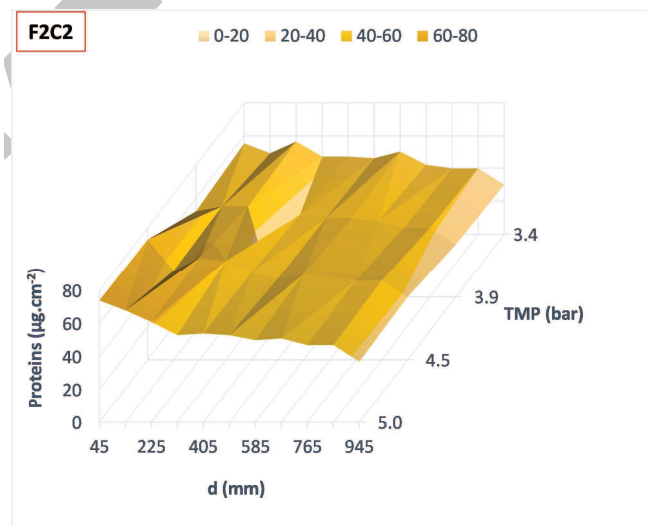
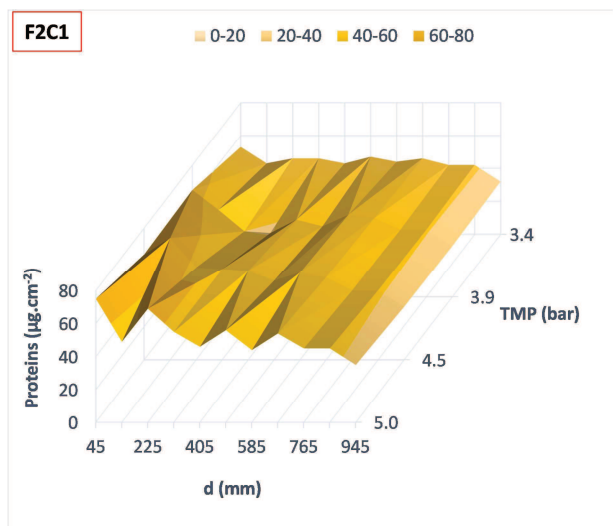
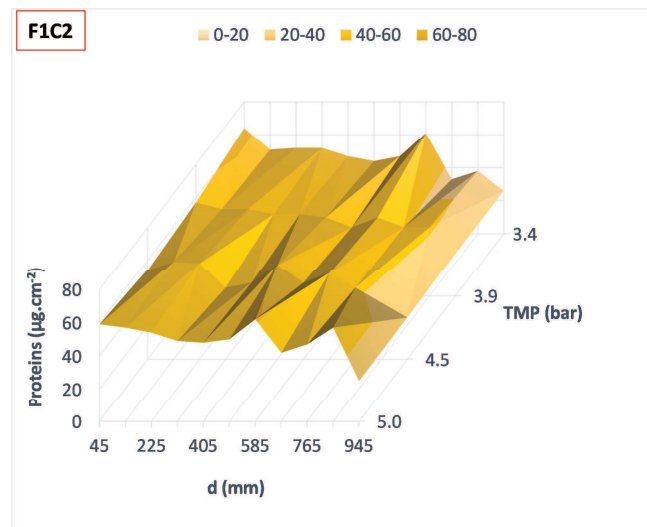
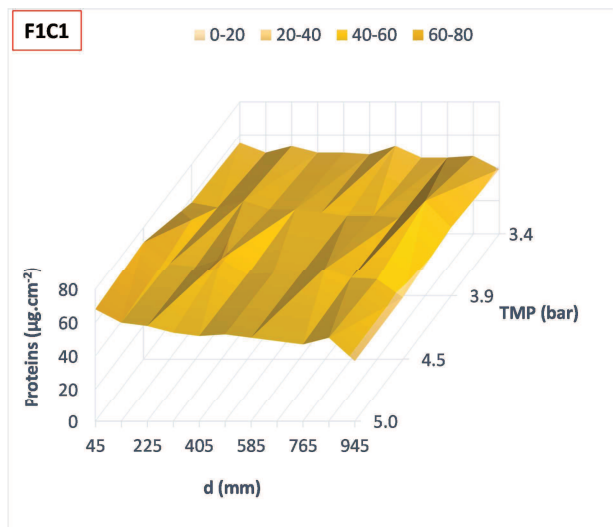


Figure 9: Evolution of flux in skim milk according to NaOCl dose received by the spiral membrane



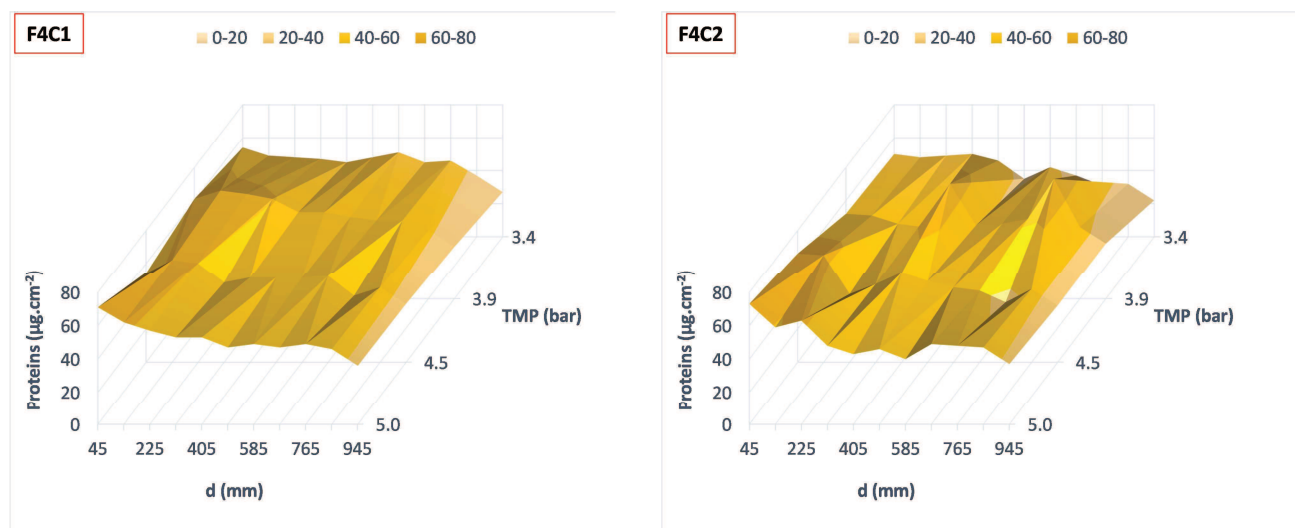
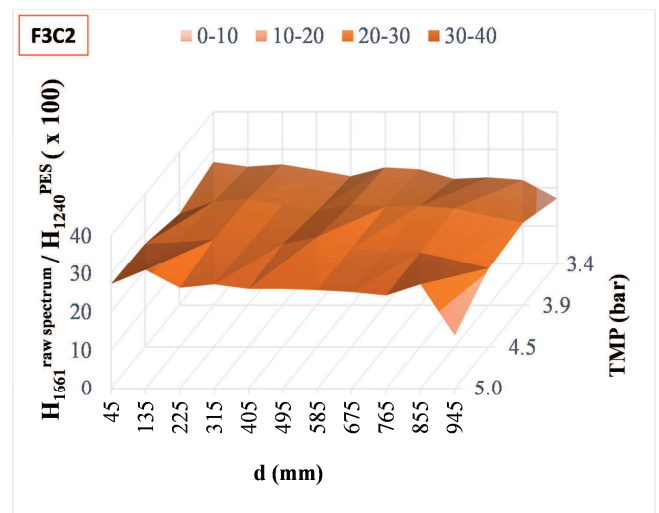
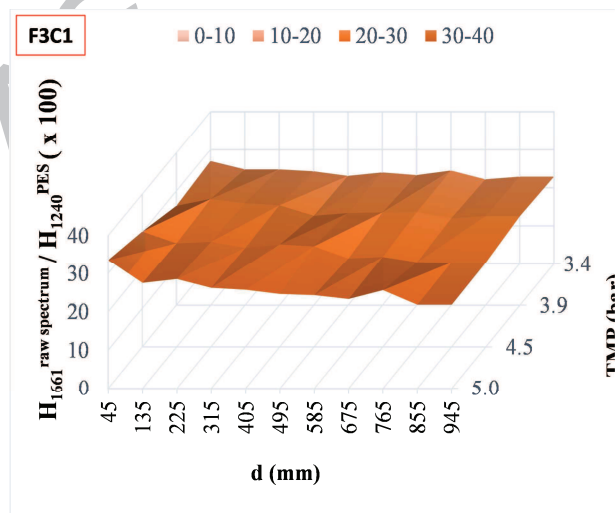
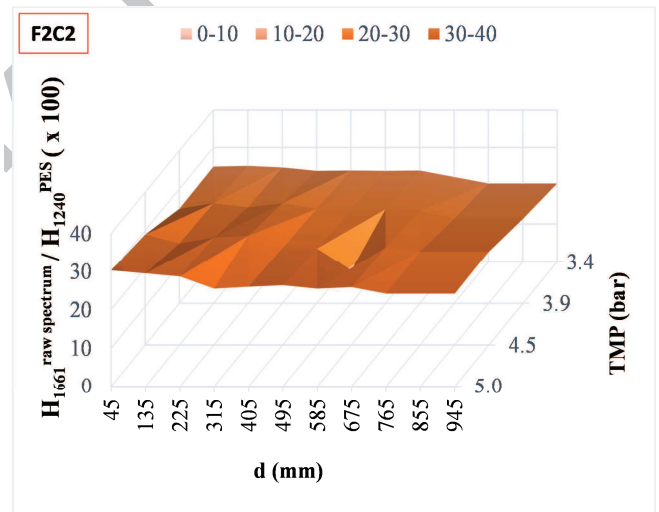
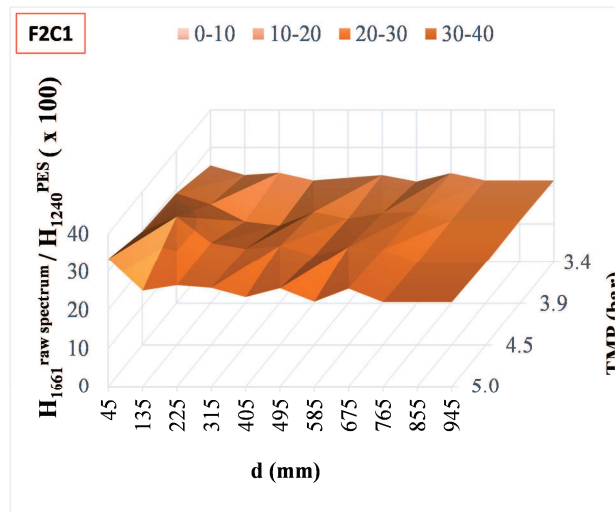
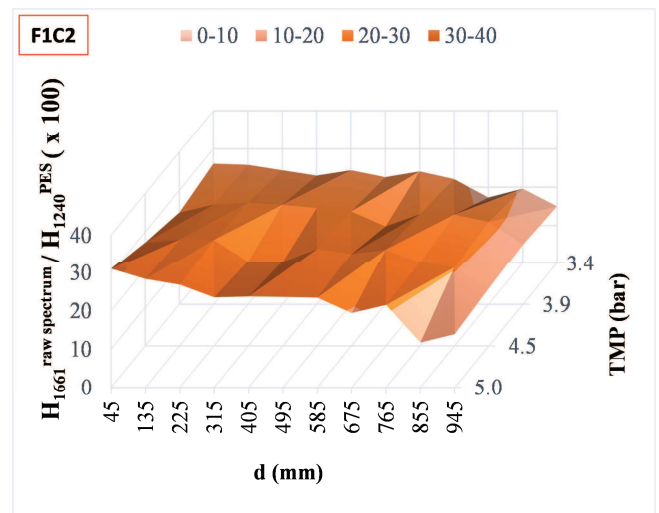
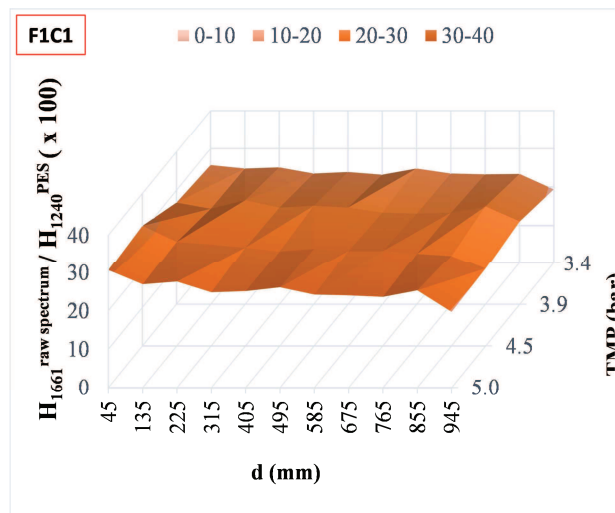


Figure 10. Mapping of the protein irreversible deposit in the spiral membrane determined from FTIR-ATR quantification (protein amount in $\mu\text{g}\cdot\text{cm}^{-2}$) according to the location in the spiral membrane. The local TMP is calculated from the assumption of a linear pressure drop decrease. The membrane labels are defined on **Figure 8**. TMP decreases from the inlet to the outlet of the spiral membrane. d is the distance from the permeate axis ($d=0$) for a membrane sheet.



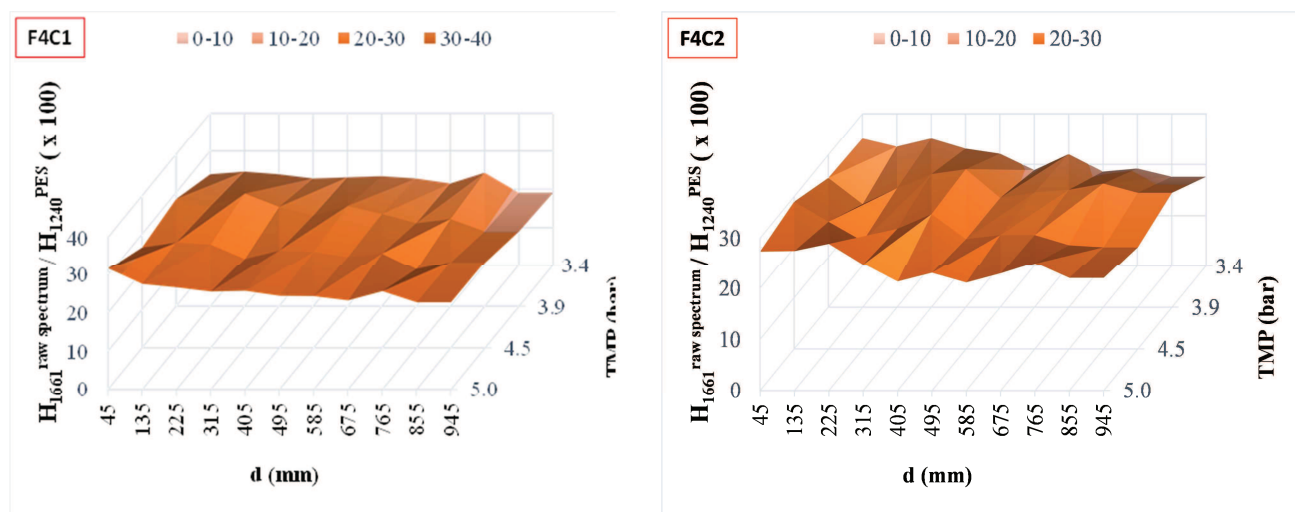
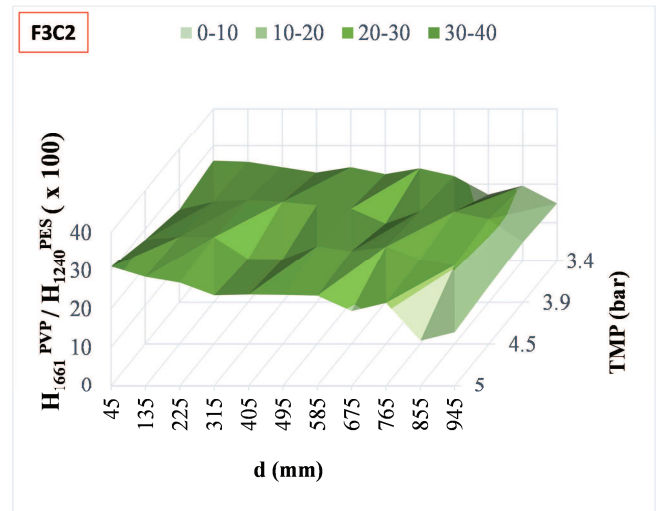
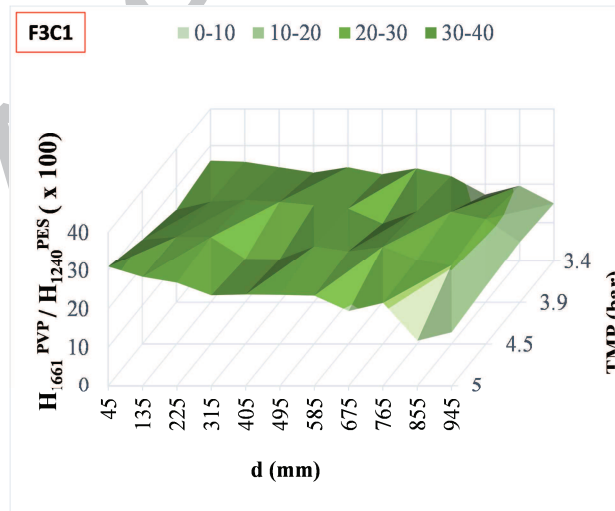
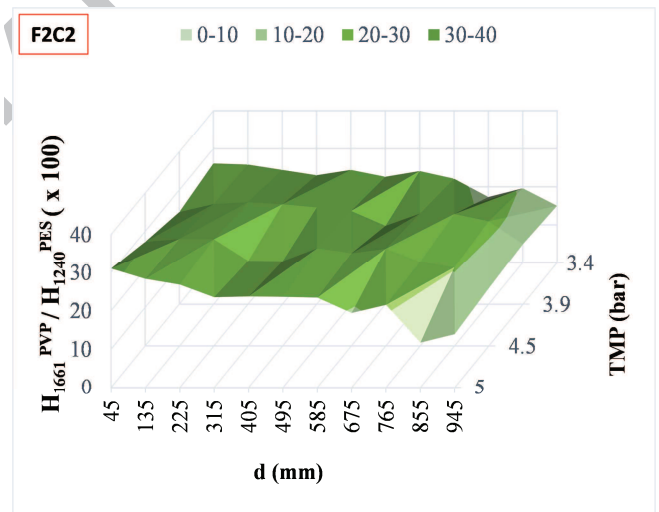
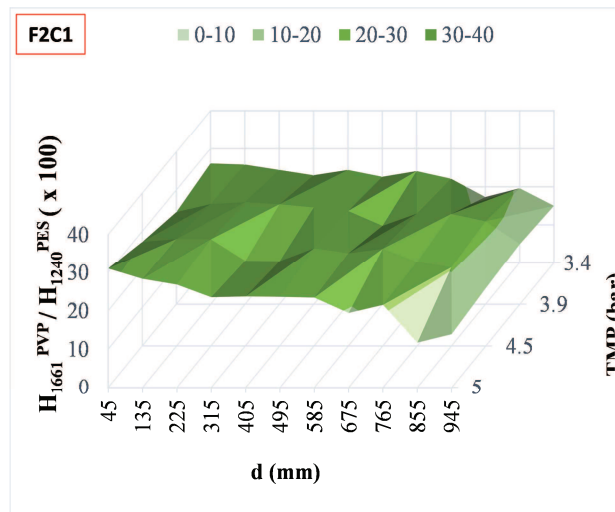
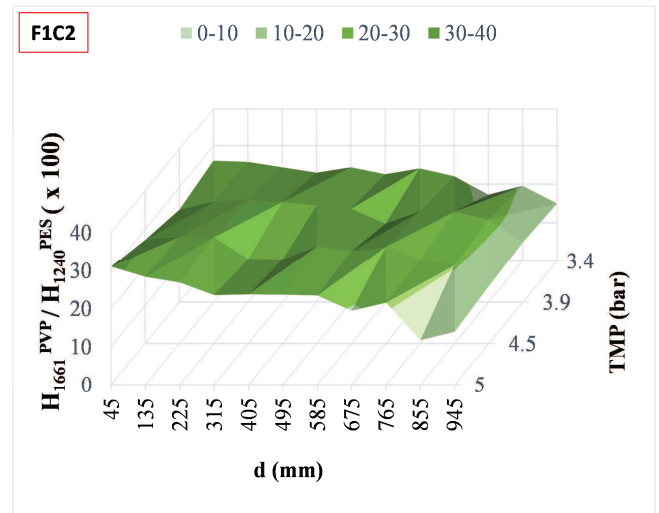
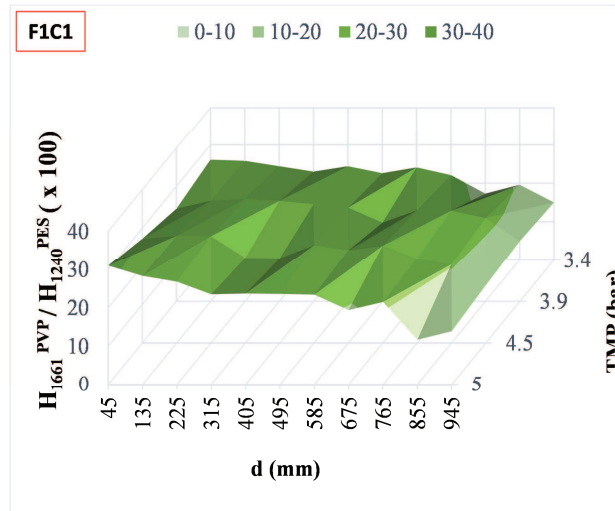


Figure 11 Mapping of $H_{1661}^{\text{raw spectrum}} / H_{1240}^{\text{PES}}$ obtained from FTIR-ATR according to the location in the spiral membrane. The local TMP is calculated from the assumption of a linear pressure drop decrease. The membrane labels are defined on **Figure 8**. TMP decreases from the inlet to the outlet of the spiral membrane. d is the distance from the permeate axis ($d=0$) for a membrane sheet.



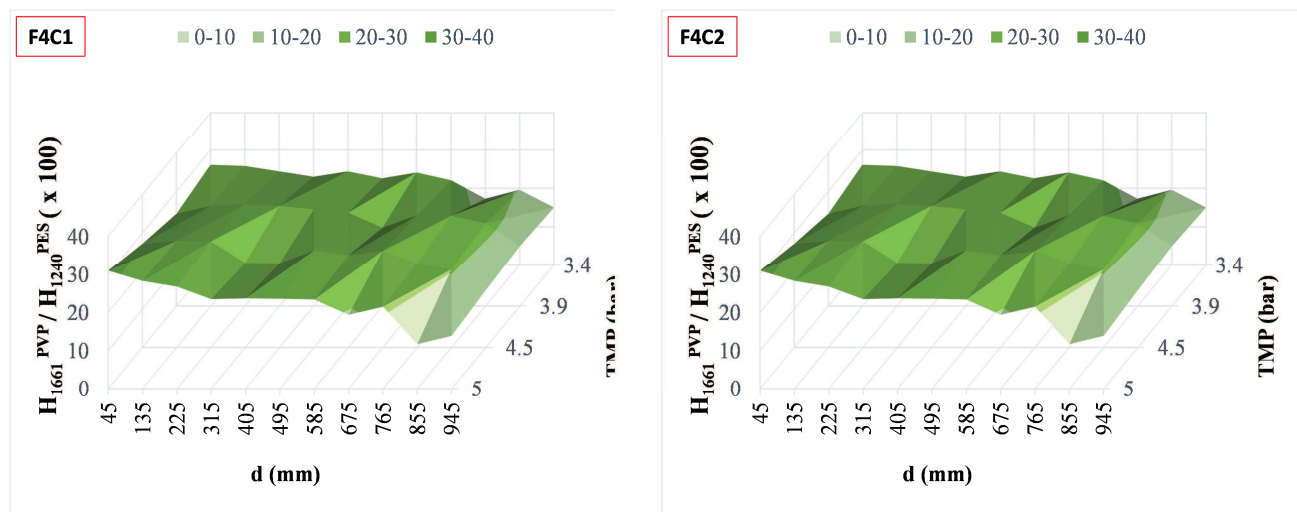
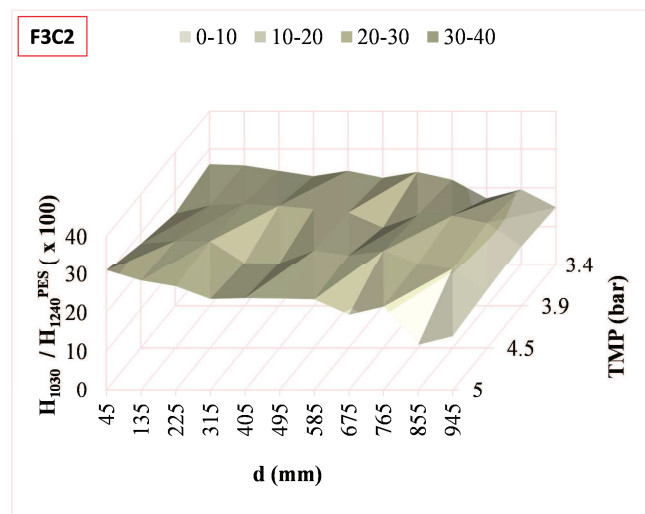
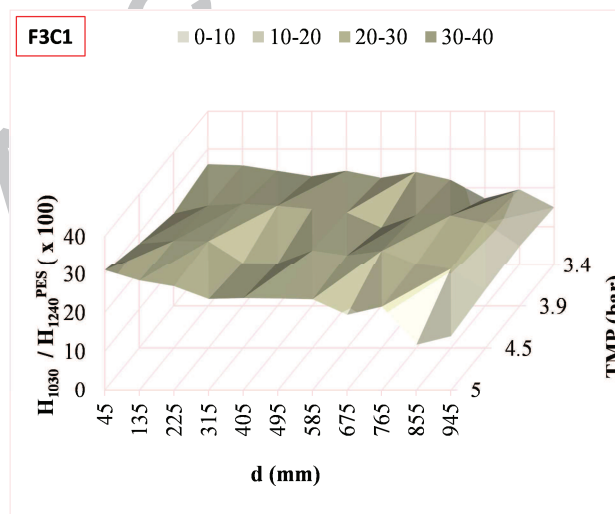
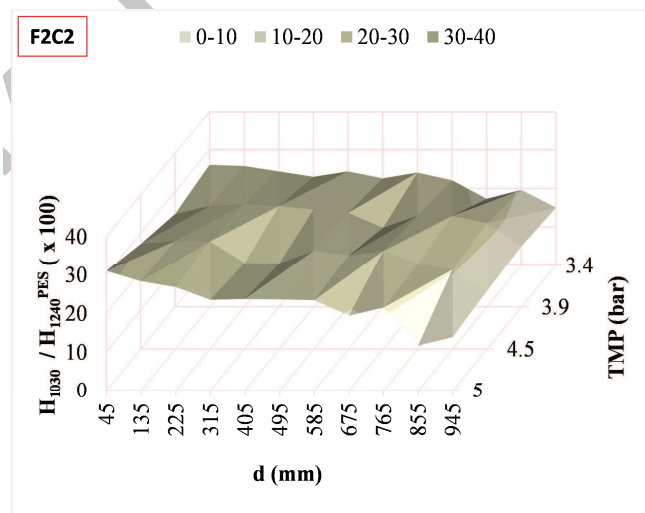
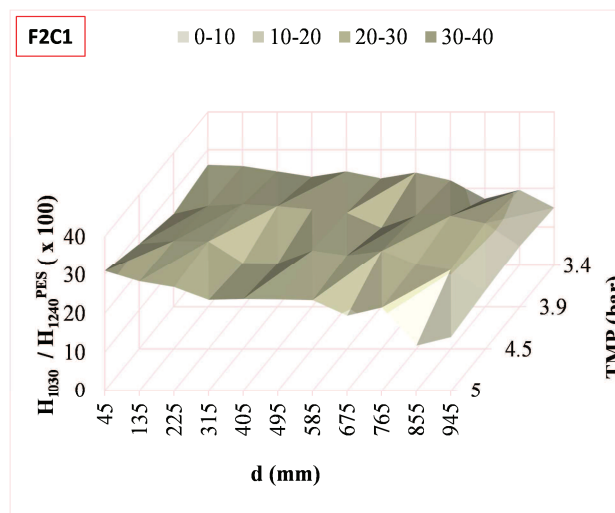
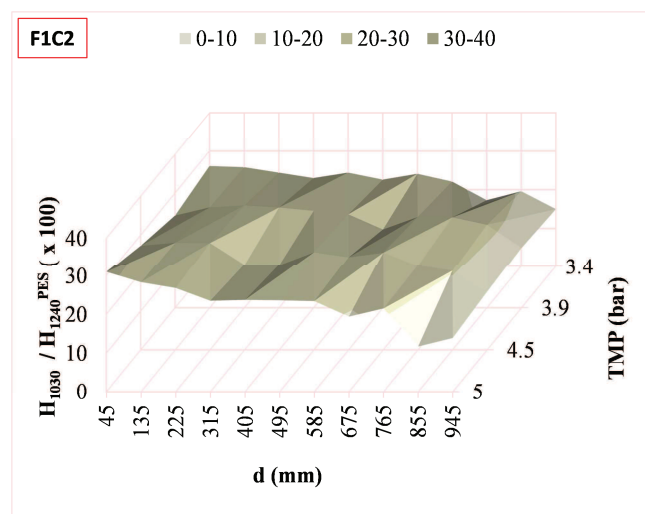
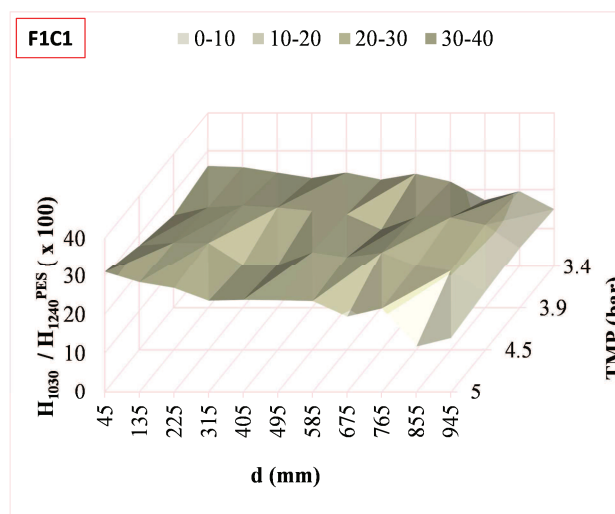


Figure 12. Mapping of $H_{1661}^{PVP}/H_{1240}^{PES}$ obtained from **equation 3** according to the location in the spiral membrane. The local TMP is calculated from the assumption of a linear pressure drop decrease. The membrane labels are defined on **Figure 8**. TMP decreases from the inlet to the outlet of the spiral membrane. d is the distance from the permeate axis ($d=0$) for a membrane sheet



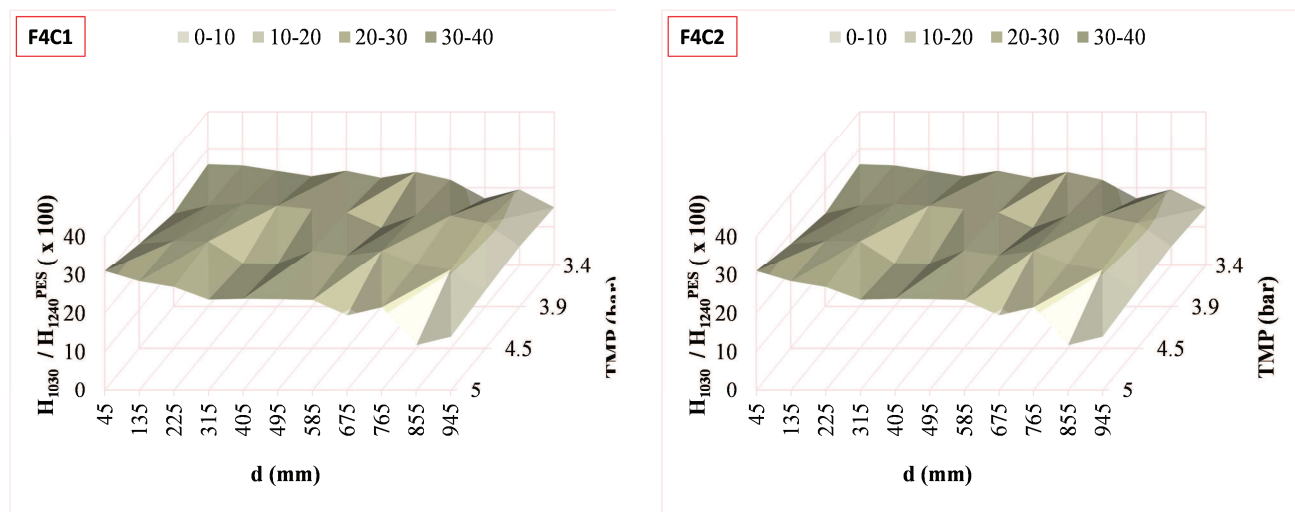


Figure 13. Mapping of H_{1030}/H_{1240}^{PES} according to the location in the spiral membrane. The local TMP is calculated from the assumption of a linear pressure drop decrease. The membrane labels are defined on **Figure 8**. TMP decreases from the inlet to the outlet of the spiral membrane. d is the distance from the permeate axis ($d=0$) for a membrane sheet

Highlights

- - evidencing PES/PVP membrane degradation by FTIR despite presence of protein fouling
-
- - methodology of treatment of FTIR spectra to reveal membrane degradation due to NaOCl
-
- - application to mapping of PVP degradation due to NaOCl in a spiral membrane
-
- - application to mapping of PES degradation due to NaOCl in a spiral membrane

ACCEPTED MANUSCRIPT